

GITR-FC FUSION PROTEIN INHIBITS GITR TRIGGERING AND PROTECTS FROM THE
INFLAMMATORY RESPONSE FOLLOWING SPINAL CORD INJURY.

Giuseppe Nocentini¹, Salvatore Cuzzocrea¹, Tiziana Genovese, Rodolfo Bianchini, Emanuela
Mazzon, Simona Ronchetti, Emanuela Esposito, Di Paola Rosanna, Placido Bramanti and Carlo
Riccardi

Dipartimento di Medicina Clinica e Sperimentale, Sezione di Farmacologia, Tossicologia e
Chemioterapia, Università di Perugia, Italy (G.N., R.B., C.R.); Dipartimento Clinico e
Sperimentale di Medicina e Farmacologia, Torre Biologica, Policlinico Universitario,
98123 Messina, Italy (S.C.); IRCCS Centro Neurolesi "Bonino-Pulejo", Messina, Italy
(T.G., E.M., E.E., D.P.R., P.B.)

Running title: GITR-Fc in SCI

Corresponding author:

Salvatore Cuzzocrea

Dipartimento Clinico e Sperimentale di Medicina e Farmacologia,

Torre Biologica, Policlinico Universitario,

98123 Messina, Italy

phone no: +39 090 2213644

fax no: +39 090 2213300

e-mail address: salvator@unime.it

Statistic

Number of text pages 33

Number of Tables 0

Number of Figures 11

Number of References 37

Number of word

- In the abstract: 193
- In the introduction: 489
- In the discussion: 1125

Non-standard abbreviations

APC, antigen presenting cells; BBB scale data, Basso, Beattie, and Bresnahan hind limb locomotor rating scale; CFSE, carboxyfluorescein diacetate succinimidyl ester; DC, dendritic cell; FCS, Foetal calf serum; GITR, Glucocorticoid-Induced TNFR-Related gene/protein; GITR^{-/-}, GITR deficient (mice); GITR^{+/+}, wild type (mice); GITR-Fc, fusion protein including the extracellular domain of GITR; GITRL, GITR ligand; IL, interleukin; iNOS, inducible NO synthase; PBS, phosphate buffered saline; SCI, spinal cord injury; TNFRSF, Tumor Necrosis Factor Receptor Superfamily; TUNEL, Terminal Deoxynucleotidyltransferase-Mediated UTP End Labeling;

ABSTRACT

Glucocorticoid-Induced Tumor necrosis factor receptor-Related (GITR) protein is a co-stimulatory molecule that plays a role in inflammation so that GITR-Fc fusion protein can exert an anti-inflammatory effect. To investigate the mechanism by which GITR-Fc exerts its effects, we first used GITR knock-out (GITR^{-/-}) mice to verify whether GITRL/GITR system played a pro-inflammatory role in the spinal cord injury (SCI) model. Notably, a less pronounced disease was induced in GITR^{-/-} as compared to GITR^{+/+} mice. We then evaluated the effect of GITR-Fc fusion protein against SCI-induced injuries in GITR^{-/-} and wild type (GITR^{+/+}) mice. Administration of GITR-Fc ameliorated SCI-induced inflammation in GITR^{+/+} mice as evaluated through: 1) histological damage and apoptosis, 2) modulation of apoptosis-related transduction factors (Bax and Bcl-2), 3) expression of inflammatory markers (nitrotyrosine, iNOS, IL-2, IL-12 and TNF- α) and 4) T lymphocyte infiltration. GITR-Fc was effective in GITR^{+/+} but not in GITR^{-/-} suggesting that, in this experimental model, its anti-inflammatory action is due to inhibition of GITR triggering and not to GITRL activation. In conclusion, GITR plays a role in SCI and administration of GITR-Fc results in amelioration of SCI severity prompting further studies on the potential anti-inflammatory properties of GITR-Fc.

INTRODUCTION

The central nervous system is sensitive to mechanical injuries causing permanent functional deficits such as the case of patients who have spinal cord injury (SCI). The mechanical forces imparted to the spinal cord cause immediate tissue disruption, with a direct axonal and neuronal injury, inducing the death of a number of neurons that to date can neither be recovered nor regenerated. Moreover, neurons continue to die for hours after SCI due to several mechanisms including excitotoxicity, vascular abnormalities and inflammatory response that can contribute to evolution of spinal cord secondary injury (Kwon et al., 2004).

Post-traumatic inflammation is determined by a number of cellular and molecular events (Carlson et al., 1998). Leukocytes are directly involved in the pathogenesis and extension of SCI (Carlson et al., 1998; Fleming et al., 2006). In fact they infiltrate the marginal zone around the injured area, release inflammatory mediators and activate endothelial cells leading to increased vascular permeability, edema formation and cell death (Kwon et al., 2004). Free radical production and lipid peroxidation is also important in the acute pathophysiology of SCI, both during the initial period of hypoperfusion and even more significantly during the period of reperfusion (Sakamoto et al., 1991). Glucocorticoid-Induced TNFR-Related (GITR) protein originally cloned in a glucocorticoid-treated hybridoma T cell line (Nocentini et al., 1997) is a protein belonging to Tumor Necrosis Factor Receptor Superfamily (TNFRSF). It is expressed in several cells and tissues, including T cells, where it acts as a co-stimulatory molecule (Ronchetti et al., 2007; Ronchetti et al., 2004; Tone et al., 2003) following activation by its ligand (GITRL), mainly expressed on antigen presenting cells (APC) and endothelial cells. GITRL/GITR system participates in the development of autoimmune diseases and potentiates response to infection and tumors (Nocentini et al., 2007b). Recent evidences suggest that physiological or pharmacological triggering of GITR exacerbates acute and chronic inflammatory response not only due to T cell modulation but also to modulation of extravasation and innate immunity (Krausz et al., 2007). Moreover, treating animals with GITR-Fc fusion protein ameliorates inflammation (Cuzzocrea et al., 2006; Cuzzocrea et al., 2007). The main

mechanism of action of GITR-Fc used as anti-inflammatory compound is still unknown, potentially being either inhibition of GITR triggering and/or stimulation of GITRL. In fact, GITRL can activate cytoplasmatic signals upon GITR binding and privilege the development of tolerogenic dendritic cells (DCs)(Agostini et al., 2005; Baltz et al., 2007; Grohmann et al., 2007; Shin et al., 2005). Establishing the main mechanism of action of GITR-Fc is crucial to plan treatment of diseases with different pathogenesis.

We here show that GITR plays a role in the modulation of secondary injury in a SCI model, demonstrating that GITR deficient ($\text{GITR}^{-/-}$) mice develop weaker SCI-induced injury and that GITR-Fc weakens SCI-induced injury. Moreover, GITR-Fc is active in $\text{GITR}^{+/+}$ but not in $\text{GITR}^{-/-}$ mice, although $\text{GITR}^{-/-}$ mice develop a significantly reduced pathology, suggesting that the main mechanism of action of GITR-Fc is the inhibition of GITR triggering.

MATERIAL AND METHODS

Animals

Sv129 mice (8-9 weeks old, 22-24 g, of both sexes, H-2^b) with a targeted disruption of GTR gene (GTR^{-/-}) and wild-type controls (GTR^{+/+}) were used (Ronchetti et al., 2002). Animal care was in compliance with regulations in Italy (D.M. 116192), Europe (O.J. of E.C. L 358/1 12/18/1986), and USA (Animal Welfare Assurance No A5594-01, Department of Health and Human Services, USA).

Spinal cord injury (SCI)

Mice were anesthetized using chloral hydrate (400 mg/kg body weight). A longitudinal incision was made on the midline of the back, exposing the paravertebral muscles. These muscles were dissected away exposing T5-T8 vertebrae. The spinal cord was exposed via a four-level T5-T8 laminectomy and SCI was produced by extradural compression of the spinal cord using an aneurysm clip with a closing force of 24 g. In all injured groups, the spinal cord was compressed for 1 min. Sham animals were only subjected to laminectomy. Following surgery, 1.0 cc of saline was administered subcutaneously in order to replace the blood volume lost during the surgery. During recovery from anesthesia, the mice were placed on a warm heating pad and covered with a warm towel. The mice were individually housed in a temperature-controlled room at 27°C for a survival period of 10 days. Food and water were provided to the mice ad libitum. During this time period, the animals' bladders were manually voided twice a day until the mice were able to regain normal bladder function.

Mini-osmotic pump implantation and fusion protein delivery.

Alzet pumps are precision drug administration tools that were used to deliver fusion proteins at a constant rate. In particular, we implanted Alzet Model 2004 miniosmotic pumps (Charles River Milan Italy) 3 hours after SCI, as previously described (Cuzzocrea et al., 2007). The pumping rate was 1 µl/h (± 0.15 µl/h) and the reservoir volume was 200 µl.

Experimental groups

Mice were randomly allocated into the following groups: 1) SCI-GITR^{+/+} group: mice were subjected to SCI and received saline by mini-osmotic pump; 2) SCI-GITR^{-/-} group: mice were subjected to SCI and received saline by mini-osmotic pump; 3) control GITR^{+/+} group (sham): GITR^{+/+} mice were subjected to the surgical procedures as the above except that the aneurysm clip was not applied and received saline by mini-osmotic pump; 4) control GITR^{-/-} group (sham): GITR^{-/-} mice were subjected to the surgical procedures as the above groups except that the aneurysm clip was not applied and received saline by mini-osmotic pump; 5) GITR-Fc-treated SCI-GITR^{+/+} group: GITR^{+/+} mice were subjected to SCI and received GITR-Fc (6.25 µg/mouse) by mini-osmotic pump. GITR-Fc was purchased from Alexis and is a dimer of a fusion protein formed by the extracellular domain of GITR and the Fc portion of human IgG1; 6) Fc-treated SCI-GITR^{+/+} group: GITR^{+/+} mice were subjected to SCI and received Fc control (6.25 µg/mouse) by mini-osmotic pump. Fc was purchased from Alexis and is a dimer of a fusion protein formed by the Fc portion of human IgG1. 7) GITR-Fc-treated SCI-GITR^{-/-} group: GITR^{-/-} mice were subjected to SCI and received GITR-Fc (6.25 µg/mouse) by mini-osmotic pump. 8) GITR-Fc-treated GITR^{+/+} group: GITR^{+/+} mice were subjected to the surgical procedures as the above groups except that the aneurysm clip was not applied and received GITR-Fc (6.25 µg/mouse) by mini-osmotic pump. 9) Fc-treated GITR^{+/+} group: GITR^{+/+} mice were subjected to the surgical procedures as the above groups except that the aneurysm clip was not applied and received Fc control (6.25 µg/mouse) by mini-osmotic pump. 10) GITR-Fc-treated GITR^{-/-} group: GITR^{-/-} mice were subjected to SCI and received GITR-Fc (6.25 µg/mouse) by mini-osmotic pump.

Mice from each group were sacrificed 24 h following SCI in order to collect samples for the evaluation of the parameters as described below. In each experiment, 5 mice/group were treated with the exception of groups 8, 9 and 10 (1-2 mice groups). Three experiments were performed. No

differences were observed in the histologies between groups 8, 9 and 10 and the respective sham-treated controls (groups 1-4) concerning each of the parameter studied.

In the experiments investigating the motor score, the animals were observed for 10 days after SCI.

In each experiment, 8 mice/group were treated and three experiments were performed.

Grading of motor disturbance.

The motor function of mice subjected to compression trauma was assessed once a day for 10 days after injury. Recovery from motor disturbance was graded using the modified murine Basso, Beattie, and Bresnahan (BBB) (Basso et al., 1995) hind limb locomotor rating scale (Joshi and Fehlings, 2002a; Joshi and Fehlings, 2002b). The following criteria were considered: 0=No hind limb movement; 1=Slight (<50% range of motion) movement of 1-2 joints; 2=Extensive (>50% range of motion) movement of 1 joint and slight movement of one other joint; 3=Extensive movement of 2 joints; 4=Slight movement in all 3 joints; 5=Slight movement of 2 joints and extensive movement of 1 joint; 6=Extensive movement of 2 joints and slight movement of 1 joint; 7=Extensive movement of all 3 joints; 8=Sweeping without weight support or plantar placement and no weight support; 9=Plantar placement with weight support in stance only or dorsal stepping with weight support; 10=Occasional (0-50% of the time) weight-supported plantar steps and no coordination (Front/hind limb coordination); 11=Frequent (50-94% of the time) to consistent (95-100% of the time) weight-supported plantar steps and no coordination; 12=Frequent to consistent weight-supported plantar steps and occasional coordination; 13=Frequent to consistent weight-supported plantar steps and frequent coordination; 14=Consistent weight-supported plantar steps, consistent coordination and predominant paw position is rotated during locomotion (lift off and contact) or frequent plantar stepping, consistent coordination and occasional dorsal stepping; 15=Consistent plantar stepping and coordination, no/occasional toe clearance, paw position is parallel at initial contact; 16=Consistent plantar stepping and coordination (Front/hind limb

coordination) and frequent toe clearance and predominant paw position is parallel at initial contact and rotated at lift off; 17=Consistent plantar stepping and coordination and frequent toe clearance and predominant paw position is parallel at initial contact and lift off; 18=Consistent plantar stepping and coordination and consistent toe clearance and predominant paw position is parallel at initial contact and rotated at lift off; 19=Consistent plantar stepping and coordination and consistent toe clearance and predominant paw position is parallel at initial contact and lift off; 20=Consistent plantar stepping, coordinated gait, consistent toe clearance, predominant paw position is parallel at initial contact and lift off and trunk instability; 21=Consistent plantar stepping, coordinated gait, consistent toe clearance, predominant paw position is parallel at initial contact and lift off and trunk stability.

Immunohistochemistry

Twenty-four hours after SCI, the tissues were fixed in 10% (w/v) PBS-buffered formaldehyde and 8 mm sections were prepared from paraffin embedded tissues. After deparaffinisation, endogenous peroxidase was quenched with 0.3% (v/v) hydrogen peroxide in 60% (v/v) methanol for 30 min. The sections were permeabilized with 0.1% (w/v) Triton X-100 in PBS for 20 min. Non-specific adsorption was minimized by incubating the section in 2% (v/v) normal goat serum in PBS for 20 min. Endogenous biotin or avidin binding sites were blocked by sequential incubation for 15 min with biotin and avidin (DBA), respectively. Sections were incubated overnight with anti-nitrotyrosine rabbit Ab, anti-iNOS Ab rat, anti-Fas-ligand monoclonal antibody, anti-Bax rabbit Ab, anti-Bcl-2 Ab, anti-TNF- α Ab, anti-IL-2 Ab, anti-IL-12 Ab, anti-CD4 Ab, or anti-CD8 Ab. Dilution of Abs was 1:100 or 1:500 v/v in PBS as previously specified (Cuzzocrea et al., 2008). Sections were washed with PBS, and incubated with secondary antibody. Specific labeling was detected with a biotin-conjugated goat anti-rabbit IgG and avidin-biotin peroxidase complex (DBA). To verify binding specificity some sections were incubated with only the secondary antibody (no primary). Immunohistochemical photographs (n=5 from each sample collected from each mouse in each

experimental group) were assessed by densitometry as previously described (Shea, 1994) by using Optilab Graftek software.

Terminal Deoxynucleotidyltransferase-Mediated UTP End Labeling (TUNEL) Assay.

TUNEL assay is a technique revealing double strand breaks and used to detect apoptotic cells. It was conducted by using a TUNEL detection kit according to the manufacturer's instructions (Apotag, HRP kit DBA, Milano, Italy). Briefly, sections were incubated with 15 µg/ml proteinase K for 15 min at room temperature and then washed with PBS. Endogenous peroxidase was inactivated by 3% H₂O₂ for 5 min at room temperature and then washed with PBS. Sections were dipped into terminal deoxynucleotidyltransferase (TdT) buffer containing deoxynucleotidyl transferase and biotinylated dUTP in TdT buffer, incubated in a humid atmosphere at 37°C for 90 min, and then washed with PBS. The sections were incubated at room temperature for 30 min with anti-horseradish peroxidase-conjugated antibody, and the signals were visualized with diaminobenzidine.

Light microscopy

Spinal cord biopsies were taken 24 h following trauma. The biopsies were fixed for 24 h in paraformaldehyde solution (4 % in PBS 0.1 M) at room temperature, dehydrated by graded ethanol and embedded in Paraplast (Sherwood Medical, Mahwah, NJ). Tissue sections (thickness 5 µm) were deparaffinized with xylene, stained with Haematoxylin/Eosin (H&E) and Luxol Fast Blue staining (used to assess demyelination) and studied using light microscopy (Dialux 22 Leitz). Damaged neurons were counted and the histopathologic changes of the gray matter were scored on a 6-point scale (Sirin et al., 2002): 0, no lesion observed, 1, gray matter contained 1 to 5 eosinophilic neurons; 2, gray matter contained 5 to 10 eosinophilic neurons; 3, gray matter contained more than 10 eosinophilic neurons; 4, small infarction (less than one third of the gray matter area); 5, moderate infarction (one third to one half of the gray matter area); 6, large

infarction (more than half of the gray matter area). The scores from all the sections from each spinal cord were averaged to give a final score for an individual mouse. All the histological studies were performed in a blinded fashion.

T cell proliferation by CFSE labeling

CFSE labeling technique reveals cells undergoing cell doublings during in vitro test. In fact, cells are labeled at time 0, cultured in vitro, and, at the end of the culture period, are studied by flow cytometry to evaluate the amount of CFSE present. More they have proliferated, less CFSE is present in the cells. Briefly, T lymphocytes were obtained from spleen or axillary, brachial, maxillary and inguinal lymph node of $GITR^{+/+}$ and $GITR^{-/-}$ mice. Cells were resuspended at 1×10^6 cells/ml in pre-warmed (37°C) PBS with 0.1% BSA. Freshly prepared CFSE (Molecular Probes) was added to a final concentration of $10 \mu\text{M}$ and the cells were incubated for 10 min at 37°C . Excess CFSE was quenched by adding 5 volumes of ice-cold RPMI 1640 medium containing 10% FBS and incubating the cells for 5 min on ice. CFSE-labelled cells were then washed three times with RPMI 1640 medium containing 10% FBS and cultured with the indicated stimuli.

0.5×10^6 cells/ml cells were cultured in RPMI 1640 medium supplemented with 10% heat-inactivated FCS, streptomycin ($100 \mu\text{g/ml}$), 10 mM Hepes, 0.1 % non-essential amino acids, 1 mM sodium pyruvate and $50 \mu\text{M}$ 2-ME. Goat anti-CD3 ϵ mAb (clone 145-2C11, BD Biosciences PharMingen, San Diego, CA) was added in soluble form and the concentration reported. GITR-Fc and Fc-isotype control (Alexis, Lausen, Switzerland) were added at a final concentration of $2 \mu\text{g/ml}$. Seventy two hour later, the percentage of cells that have performed at least 1 cell cycle was evaluated through flow cytometry, conducted on a Beckman Coulter EPICS XL-MCL running FCS Express 3.0 De Novo analysis software.

Materials

Unless otherwise stated, all compounds were obtained from Sigma-Aldrich Company Ltd. (Milan, Italy). GITR-Fc was purchased from Alexis. All stock solutions were prepared in non-pyrogenic saline (0.9% NaCl; Baxter, Italy) or 10% DMSO.

Statistical evaluation

All values in the figures and text are expressed as mean \pm standard error of the mean (SEM). In the experiments involving histology or immunohistochemistry, shown figures are representative of at least three experiments performed on different experimental days. The results were analyzed by one-way ANOVA followed by a Bonferroni post-hoc test for multiple comparisons. A p-value of less than 0.05 was considered significant. BBB scale data were analyzed by the Mann-Whitney test and considered significant when p-value was less than 0.05.

RESULTS

The absence of GITR reduces the severity of spinal cord trauma

We induced spinal cord injury (SCI) by 1 minute of extradural compression and evaluated if GITRL/GITR system modulates the loss of motor function, by using the modified BBB hind limb locomotor rating scale. While motor function was only slightly impaired in sham mice, GITR^{+/+} mice subjected to SCI had significant deficits in hind limb movement (Figure 1). Lighter hind limb motor disturbances were observed in mice lacking GITR (GITR^{-/-} mice)(Figure 1), suggesting that GITRL/GITR system is involved in the development of SCI lesions.

To verify if there was a correlation between the better motor score and the inflammatory response, we studied the histology of the perilesional area, 24 hours after the induction of SCI. Edema, alteration of the white matter (Figure 2c and 2c1) and a significant loss of myelin in lateral and dorsal funiculi (Figure 3c) were observed in the spinal cord tissue of GITR^{+/+} mice. Notably, the absence of GITR gene significantly reduced the extent and severity of the histological signs of SCI (Figures 2d and 2g) as well as attenuated the myelin degradation in the central part of lateral and dorsal funiculi (Figure 3d), thus indicating that lack of GITRL-GITR interaction results in reduction of inflammatory response.

Pharmacological inhibition of GITR triggering reduces the severity of spinal cord lesions

To verify whether GITR-Fc negatively modulates the secondary SCI-induced lesions, we treated SCI-GITR^{+/+} mice with a continuous infusion of GITR-Fc fusion protein. The treatment of SCI-GITR^{+/+} mice with GITR-Fc fusion protein partially reverted tissue damage (Figures 2e, 2g and 3e) giving results similar to those obtained with SCI-GITR^{-/-} mice. Treatment of SCI-GITR^{+/+} mice with the control isotype-Fc fusion protein did not reduce the histological alteration (Figure 2g and data not shown), suggesting that GITR-Fc has a specific activity. Moreover, GITR-Fc infusion into SCI-GITR^{-/-} mice did not decrease histological alteration (Figures 2f, 2g and 3f), suggesting the

therapeutic effect in SCI-GITR^{+/+} is due to an antagonist effect against GITR triggering more than to GITRL triggering.

Genetic and pharmacological inhibition of GITR triggering counters nitrotyrosine formation and iNOS expression

We next investigated whether GITR triggering inhibition modulated peroxynitrite formation and/or other nitrogen derivatives. To this aim, nitrotyrosine, a specific marker of nitrosative stress, and inducible NO synthase (iNOS) were measured by immunohistochemical analysis. Sections of spinal cord from sham-operated mice did not stain for nitrotyrosine (Figures 4a and b) or iNOS (Figures 5a and 5b), whereas spinal cord sections obtained from SCI-GITR^{+/+} mice exhibited positive staining for nitrotyrosine (Figure 4c) and iNOS (Figure 5c). The positive staining was mainly localized in inflammatory cells as well as in nuclei of Schwann cells of the white (wm) and gray (gm) matter. In SCI-GITR^{-/-} mice as well as in GITR-Fc-treated SCI-GITR^{+/+}, staining for nitrotyrosine (Figures 4d and 4e) and iNOS (Figures 5d and 5e) were visibly and significantly reduced when compared to SCI-GITR^{+/+} mice. Treatment of GITR^{+/+} mice with control Fc (Figures 4g and 5g) and treatment of GITR^{-/-} mice with GITR-Fc did not reduce the nitrotyrosine formation as well as iNOS expression (Figure 4g and 5g), as summarized in Figure 4g and 5g.

Genetic and pharmacological inhibition of GITR triggering negatively modulates the expression of pro-inflammatory cytokines

To test whether GITR triggering inhibition inhibits up-regulation of pro-inflammatory cytokines in SCI mice, we analyzed the presence of IL-2, IL-12 and TNF- α through the immunohistological staining. No staining resulted for either IL-2 (Figures 6a and 6b), IL-12 (Figures 7a, s1a and s1b, in supplemental material) and TNF- α (Figures 7b, s2a and s2b) in spinal cord obtained from the sham-operated mice. IL-2 (Figure 6c) and IL-12 (Figures 7a and s1c) were found in inflammatory cells as well as in nuclei of Schwann cells in wm and gm of the spinal cord tissues of SCI-GITR^{+/+} mice.

Levels of IL-2 (Figures 6d) and IL-12 (Figures 7a and s1d) were significantly attenuated in GITR^{-/-} mice subjected to SCI and in GITR-Fc-treated SCI-GITR^{+/+} mice (Figures 6e 7a and s1e). On the contrary, treatment of SCI-GITR^{-/-} mice with GITR-Fc did not further decrease IL-2 and IL-12 expression (Figures 6f, 7a and s1f). Similar results were obtained with TNF- α (Figure 7b and s2), suggesting that GITR-Fc decreases the production of pro-inflammatory cytokines that inhibit GITR triggering.

Pharmacological inhibition of GITR triggering negatively modulates T cell proliferation.

GITR is a costimulatory molecule in T cells, resulting in increased T cell activation and proliferation. When T cells are cultured together with other cells of lymphoid organs, GITRL expressed on APC may increase proliferation of anti-CD3-activated T cells. So we hypothesized that, if GITR-Fc acts by inhibiting GITR stimulation, its addition should in turn inhibit cell proliferation. In fact, when cells from spleen and lymph nodes were CFSE labeled and stimulated with low doses of anti-CD3, addition of GITR-Fc inhibited cell proliferation in 3 out of 4 conditions tested, as shown in Figures 8a and 8c. In order to verify whether the effect of GITR-Fc was exclusively due to the inhibition of GITR triggering (as hypothesized on the basis of in vivo experiments) or also to activation of GITRL (expressed in T cells also), we performed a similar experiment with GITR^{-/-} cells. In these cells, GITR-Fc did not exert antiproliferative activity (Figures 8b and 8c), further supporting the conclusion that GITR-Fc inhibits cell proliferation by inhibition of GITR triggering.

Genetic and pharmacological inhibition of GITR triggering modulates apoptosis, Fas ligand expression and regulation of Bcl-2 family members.

To test whether inhibition of GITR triggering by GITR-Fc had anti-apoptotic effects, we performed a TUNEL staining. Virtually no apoptotic cells were detected in the spinal cord from sham-operated mice (Figures 9a, s3a and s3b). Tissues from SCI-GITR^{+/+} mice demonstrated dark brown apoptotic

cells (about 5 cells per field) and intercellular apoptotic fragments (Figures 9a and s3c). In contrast, tissues obtained from SCI-GITR^{-/-} mice showed a smaller number of apoptotic cells (about 1 per field)(Figures 9a and s3d). Similarly, very few apoptotic cells were observed in the spinal cord tissues collected from SCI-GITR^{+/+} mice treated with GITR-Fc fusion protein (Figures 9a and s3e). Neither treatment of GITR^{+/+} mice with control Fc nor treatment of GITR^{-/-} mice with GITR-Fc reduced or increased the presence of apoptotic cells (Figures 9a and s3f).

Since it has been demonstrated that apoptotic death of SCI is Fas-dependent (Casha et al., 2005), we evaluated the levels of Fas ligand (FasL) in our experimental system. There was no staining for FasL in spinal cord obtained from sham groups (Figures 9b, s4a and s4b) but a significant presence was observed in the spinal cord tissues collected from SCI-GITR^{+/+} mice (Figures 9b and s4c). FasL levels were significantly decreased in SCI-GITR^{-/-} mice (Figures 9b and s4d). Similarly, low levels of staining for FasL was observed in the spinal cord tissues collected from GITR-Fc-treated SCI-GITR^{+/+} mice (Figures 9b and s4e). The treatment of GITR^{+/+} mice with control Fc (Figure 9b) and the treatment of GITR^{-/-} mice with GITR-Fc (Figures 9b and s4f) did not reduce nor increase the presence of FasL in the spinal cord as compared to the respective controls, further supporting the conclusion that GITR-Fc inhibits GITR triggering and that GITRL signaling has no role in the present inflammatory model.

A similar conclusion was reached studying the modulation of Bcl-2 family members that are involved in SCI-induced apoptosis (Dong et al., 2003; Seki et al., 2003). Sections of spinal cord from sham-operated mice did not stain for Bax (Figures 9c, s5a and s5b) whereas spinal cord sections obtained from SCI-GITR^{+/+} mice exhibited a positive staining (Figures 9c and s5c). Spinal cord levels of Bax were significantly attenuated in SCI-GITR^{-/-} as compared to SCI-GITR^{+/+} mice (Figures 9c and s5d). Similarly, lightly positive staining for Bax was observed in the spinal cord tissues collected from GITR-Fc-treated SCI-GITR^{+/+} mice (Figures 9c and s5e). Once again, the treatment of GITR^{-/-} mice with control GITR-Fc (Figures 9c and s5f) and GITR^{+/+} mice with control Fc (Figure 9c) did not modulate the levels of Bax.

A basal level of Bcl-2 expression was detected in the spinal cord tissues from sham-treated $GITR^{+/+}$ and $GITR^{-/-}$ mice (Figures 9d and s6a), whereas in SCI- $GITR^{+/+}$ mice Bcl-2 levels were significantly reduced (Figures 9d and s6b). Similar Bcl-2 levels to those observed in sham-treated mice were observed in SCI- $GITR^{-/-}$ as well as in GITR-Fc-treated SCI- $GITR^{+/+}$ mice (Figures 9d, s6c and s6d). In SCI- $GITR^{-/-}$ mice, GITR-Fc did not increase Bcl-2 expression (Figures 9d and s6e).

Genetic and pharmacological inhibition of GITR-GITRL interaction reduces T cell infiltration.

The anti-inflammatory effect of GITR-Fc may be also due to inhibition of leukocyte extravasation, as suggested by previous data (Cuzzocrea et al., 2006; Cuzzocrea et al., 2004; Nocentini et al., 2007a). To evaluate if genetic and pharmacological inhibition of GITR triggering inhibits leukocyte extravasation in this inflammatory model, we looked for leukocyte infiltration by immunohistochemical staining for $CD4^{+}$ and $CD8^{+}$ T lymphocytes at the injury site. As expected, there was no staining for $CD4^{+}$ (Figures 10a and 10b) and $CD8^{+}$ (Figures 11a and 11b) T lymphocytes in spinal cord obtained from the sham groups. $CD4^{+}$ (Figure 10c) and $CD8^{+}$ (Figure 11c) cells were observed in the spinal cord tissues collected from SCI- $GITR^{+/+}$ mice. $CD4^{+}$ and $CD8^{+}$ T lymphocytes infiltrates were significantly attenuated in SCI- $GITR^{-/-}$ mice (Figures 10d and 11d, respectively) and in SCI- $GITR^{+/+}$ mice treated with GITR-Fc fusion protein (Figures 10e and 11e, respectively). Treatment of SCI- $GITR^{+/+}$ mice with control Fc (Figures 10g and 11g) and of SCI- $GITR^{-/-}$ mice with GITR-Fc (Figures 10f and 11f) did not reduce the presence of $CD4^{+}$ and $CD8^{+}$ T lymphocytes in comparison to their respective control, suggesting that GITR-Fc inhibits extravasation by impeding GITR triggering.

DISCUSSION

We here demonstrate that GITRL/GITR system participates in the development of SCI-derived lesions and that the absence (GITR^{-/-} mice) or inhibition of GITR reduces the inflammatory response secondary to SCI as shown by several parameters including histological damage, apoptosis, iNOS activity, cytokine production and T lymphocyte infiltration. It is known that the inflammatory response following SCI plays a role in progression of permanent lesions (Kwon et al., 2004) and results here confirm that a lower level of inflammation correlates with decreased motor lesions as indicated by a higher motor score in SCI-GITR^{-/-} mice. In addition, we demonstrate that antagonist GITR-Fc counters SCI-induced histological injuries and inflammation.

Development of SCI-induced lesions in GITR^{+/+} mice treated with GITR-Fc fusion protein was similar to that observed in GITR^{-/-} mice concerning all the investigated parameters. This finding confirms the efficacy of GITR-Fc as an anti-inflammatory drug, as previously seen in other experimental models (Nocentini et al., 2007a), and suggests inhibition of GITR triggering results in disease reduction.

According to published data, GITR-Fc can function in 2 ways: 1) as an antagonist that inhibits GITR triggering, 2) as an agonist that stimulates GITRL. Based on different experimental models it is well known that GITR co-stimulates a number of cells, including T lymphocytes (Cuzzocrea et al., 2005; Nocentini and Riccardi, 2005; Nocentini et al., 2007b; Patel et al., 2005; Ramirez-Montagut et al., 2006; Ronchetti et al., 2007; Ronchetti et al., 2004; Tone et al., 2003). Moreover, GITR participates in the activation of neutrophils and other cells of innate immunity playing a pro-inflammatory role in acute and chronic inflammation (Cuzzocrea et al., 2006; Cuzzocrea et al., 2007; Krausz et al., 2007). Therefore, in GITR^{+/+} mice inhibition of GITR activation by administration of GITR-Fc can account for the decreased inflammatory response. Moreover, while GITR-Fc worked efficiently in GITR^{+/+}, it did not in GITR^{-/-}, clearly indicating it acts as a receptor antagonist.

An additional possibility is that GITR-Fc activates GITRL. In fact, evidences in other experimental models suggest that GITRL can activate cytoplasmic signals in a number of cells including DC, where GITRL triggering by GITR inhibits IL-12 production and increases tryptophan catabolism thus favoring a tolerogenic phenotype that could account for a decreased inflammation (Agostini et al., 2005; Grohmann et al., 2007). Moreover, results in other studies indicate that GITRL triggering on APC promotes inflammatory response (Kim et al., 2006; Shin et al., 2003). In the present experimental model we show that a milder inflammatory response was induced in GITR^{-/-} as compared to GITR^{+/+} mice, but also that GITR-Fc administration did not exert any significative effect in SCI-GITR^{-/-} mice while was effective in SCI-GITR^{+/+}. In addition, in in vitro experiments, GITR-Fc exerted an antiproliferative activity by inhibiting GITR triggering and not acting as GITRL agonist (Figure 9). These results clearly indicate that in SCI experimental model, GITRL triggering does not play a role in the modulation of inflammation and that the main mechanism of action of GITR-Fc is to antagonize GITR triggering.

In the inflammatory response, extravasation of cells plays an important role. During inflammation, both GITR and GITRL are expressed on endothelial cells of vessels and evidences have been described suggesting that GITRL/GITR system modulates extravasation (Cuzzocrea et al., 2006; Cuzzocrea et al., 2004). In the present experimental model, T cells are reduced in the perilesional area of SCI-GITR^{-/-} and GITR-Fc-treated SCI-GITR^{+/+} mice, as compared to SCI-GITR^{+/+}. These results are in agreement with our previous observation indicating a decreased extravasation of neutrophils in GITR^{-/-} mice that correlates with a decreased expression of adhesion molecules such as ICAM-1, P-selectin and E-selectin (Cuzzocrea et al., 2006; Cuzzocrea et al., 2004). The lack of differences of cell infiltration in SCI-GITR^{-/-} and GITR-Fc treated SCI-GITR^{-/-} mice, further suggest that a role is played by GITR activation, but not by GITRL activation, and that GITR-Fc inhibits extravasation by impeding GITR triggering. In our opinion, GITR, expressed on endothelial cells, is triggered by GITRL expressed on neutrophils, monocytes and activated T lymphocytes (Krausz et al., 2007) and induces up-regulation of adhesion molecules. This hypothesis is in

agreement with other studies demonstrating that GITR triggering increases expression of adhesion molecules such as P-Selectin and E-Selectin in activated T lymphocytes (Mahesh et al., 2006). Moreover, inhibition of inflammatory cell migration in the perilesional area contributes to a decreased concentration of pro-inflammatory cytokines that is also a consequence of GITR antagonism on pro-inflammatory cells as here demonstrated for TNF- α , IL-2 and IL-12 (Figures 6 and 7). The lower level of cytokines contributes, in turn, to a lower expression of adhesion molecules and lower levels of extravasation in a positive feed-back process.

After SCI, apoptosis of neurons and oligodendrocytes is associated with axonal degeneration (Kwon et al., 2004). In fact, in SCI-GITR^{+/+} mice we observed apoptotic death in the perilesional area that was less evident in SCI-GITR^{-/-} and in GITR-Fc-treated SCI-GITR^{+/+} mice. The decreased apoptosis correlated with the modulation of transduction proteins belonging to Bcl-2 family. In particular, in SCI-GITR^{-/-} mice we observed lower expression levels of the pro-apoptotic protein Bax and higher expression levels of the anti-apoptotic protein Bcl-2. These results are in accordance with previous observations showing that SCI-induced apoptosis is Bax-dependent (Dong et al., 2003; Martin and Liu, 2002) and that overexpression of Bcl-2 protects cells from SCI (Seki et al., 2003). However, considering that for signaling of Bcl-2 family members cell localization is critical, the real contribution of these proteins to SCI-induced apoptosis has to be further investigated.

Apoptosis is favored by activation of Fas receptor, which is known to be involved in the SCI lesions (Casha et al., 2005; Demjen et al., 2004). We found higher levels of FasL in SCI-GITR^{+/+} mice as compared to GITR^{-/-} and GITR-Fc-treated SCI-GITR^{+/+} mice. Thus, GITR triggering up-regulates FasL in GITR positive cells, including activated T cells that are present in the perilesional area (Figures 10 and 11), and induces higher apoptosis level in SCI-GITR^{+/+} mice. Similar conclusions were reached by Muriglian et al., working on a Graft Versus Host experimental model, showing that GITR stimulation increases FasL expression in CD4⁺ effector T cells (Muriglian et al., 2004), and by Ramirez-Montagut et al. showing that tumor rejection elicited by GITR triggering depends on augmentation of FasL expression (Ramirez-Montagut et al., 2006). We here also demonstrate that

GITR triggering inhibition by GITR-Fc inhibits SCI-induced Bax and FasL up-regulation as well Bcl-2 down-regulation.

In conclusion, GITRL/GITR system plays a role in the inflammatory neuronal lesion secondary to SCI that can be antagonized by treatment with GITR-Fc. Moreover, those results, considering the different role of GITR in different steps of inflammatory process including cell activation, cytokine production and cell migration, prompt to further studies aimed at better defining the potential use of GITR-Fc as anti-inflammatory drug and the mechanisms responsible for GITR-Fc therapeutic effect.

REFERENCES

- Agostini M, Cenci E, Pericolini E, Nocentini G, Bistoni G, Vecchiarelli A and Riccardi C (2005) The glucocorticoid-induced tumor necrosis factor receptor-related gene modulates the response to *Candida albicans* infection. *Infect Immun* **73**(11):7502-7508.
- Baltz KM, Krusch M, Bringmann A, Brossart P, Mayer F, Kloss M, Baessler T, Kumbier I, Peterfi A, Kupka S, Kroeber S, Menzel D, Radsak MP, Rammensee HG and Salih HR (2007) Cancer immunoediting by GITR (glucocorticoid-induced TNF-related protein) ligand in humans: NK cell/tumor cell interactions. *Faseb J* **21**(10):2442-2454.
- Basso DM, Beattie MS and Bresnahan JC (1995) A sensitive and reliable locomotor rating scale for open field testing in rats. *Journal of neurotrauma* **12**(1):1-21.
- Carlson SL, Parrish ME, Springer JE, Doty K and Dossett L (1998) Acute inflammatory response in spinal cord following impact injury. *Exp Neurol* **151**(1):77-88.
- Casha S, Yu WR and Fehlings MG (2005) FAS deficiency reduces apoptosis, spares axons and improves function after spinal cord injury. *Exp Neurol* **196**(2):390-400.
- Cuzzocrea S, Ayroldi E, Di Paola R, Agostini M, Mazzon E, Bruscoli S, Genovese T, Ronchetti S, Caputi AP and Riccardi C (2005) Role of glucocorticoid-induced TNF receptor family gene (GITR) in collagen-induced arthritis. *Faseb J* **19**(10):1253-1265.
- Cuzzocrea S, Bruscoli S, Mazzon E, Crisafulli C, Donato V, Di Paola R, Velardi E, Esposito E, Nocentini G and Riccardi C (2008) Peroxisome proliferator-activated receptor-alpha contributes to the anti-inflammatory activity of glucocorticoids. *Mol Pharmacol* **73**(2):323-337.
- Cuzzocrea S, Nocentini G, Di Paola R, Agostini M, Mazzon E, Ronchetti S, Crisafulli C, Esposito E, Caputi AP and Riccardi C (2006) Proinflammatory role of glucocorticoid-induced TNF receptor-related gene in acute lung inflammation. *J Immunol* **177**(1):631-641.
- Cuzzocrea S, Nocentini G, Di Paola R, Mazzon E, Ronchetti S, Genovese T, Muia C, Caputi AP and Riccardi C (2004) Glucocorticoid-induced TNF receptor family gene (GITR) knockout

- mice exhibit a resistance to splanchnic artery occlusion (SAO) shock. *J Leukoc Biol* **76**(5):933-940.
- Cuzzocrea S, Ronchetti S, Genovese T, Mazzon E, Agostini M, Di Paola R, Esposito E, Muia C, Nocentini G and Riccardi C (2007) Genetic and pharmacological inhibition of GITR-GITRL interaction reduces chronic lung injury induced by bleomycin instillation. *Faseb J* **21**(1):117-129.
- Demjen D, Klussmann S, Kleber S, Zuliani C, Stieltjes B, Metzger C, Hirt UA, Walczak H, Falk W, Essig M, Edler L, Krammer PH and Martin-Villalba A (2004) Neutralization of CD95 ligand promotes regeneration and functional recovery after spinal cord injury. *Nat Med* **10**(4):389-395.
- Dong H, Fazzaro A, Xiang C, Korsmeyer SJ, Jacquin MF and McDonald JW (2003) Enhanced oligodendrocyte survival after spinal cord injury in Bax-deficient mice and mice with delayed Wallerian degeneration. *J Neurosci* **23**(25):8682-8691.
- Fleming JC, Norenberg MD, Ramsay DA, Dekaban GA, Marcillo AE, Saenz AD, Pasquale-Styles M, Dietrich WD and Weaver LC (2006) The cellular inflammatory response in human spinal cords after injury. *Brain* **129**(Pt 12):3249-3269.
- Grohmann U, Volpi C, Fallarino F, Bozza S, Bianchi R, Vacca C, Orabona C, Belladonna ML, Ayroldi E, Nocentini G, Boon L, Bistoni F, Fioretti MC, Romani L, Riccardi C and Puccetti P (2007) Reverse signaling through GITR ligand enables dexamethasone to activate IDO in allergy. *Nat Med* **13**(5):579-586.
- Joshi M and Fehlings MG (2002a) Development and characterization of a novel, graded model of clip compressive spinal cord injury in the mouse: Part 1. Clip design, behavioral outcomes, and histopathology. *Journal of neurotrauma* **19**(2):175-190.
- Joshi M and Fehlings MG (2002b) Development and characterization of a novel, graded model of clip compressive spinal cord injury in the mouse: Part 2. Quantitative neuroanatomical

- assessment and analysis of the relationships between axonal tracts, residual tissue, and locomotor recovery. *Journal of neurotrauma* **19**(2):191-203.
- Kim WJ, Bae EM, Kang YJ, Bae HU, Hong SH, Lee JY, Park JE, Kwon BS, Suk K and Lee WH (2006) Glucocorticoid-induced tumour necrosis factor receptor family related protein (GITR) mediates inflammatory activation of macrophages that can destabilize atherosclerotic plaques. *Immunology* **119**(3):421-429.
- Krausz LT, Bianchini R, Ronchetti S, Fettucciari K, Nocentini G and Riccardi C (2007) GITR-GITRL system, a novel player in shock and inflammation. *ScientificWorldJournal* **7**:533-566.
- Kwon BK, Tetzlaff W, Grauer JN, Beiner J and Vaccaro AR (2004) Pathophysiology and pharmacologic treatment of acute spinal cord injury. *Spine J* **4**(4):451-464.
- Mahesh SP, Li Z, Liu B, Fariss RN and Nussenblatt RB (2006) Expression of GITR ligand abrogates immunosuppressive function of ocular tissue and differentially modulates inflammatory cytokines and chemokines. *Eur J Immunol* **36**(8):2128-2138.
- Martin LJ and Liu Z (2002) Injury-induced spinal motor neuron apoptosis is preceded by DNA single-strand breaks and is p53- and Bax-dependent. *J Neurobiol* **50**(3):181-197.
- Muriglian SJ, Ramirez-Montagut T, Alpdogan O, Van Huystee TW, Eng JM, Hubbard VM, Kochman AA, Tjoe KH, Riccardi C, Pandolfi PP, Sakaguchi S, Houghton AN and Van Den Brink MR (2004) GITR activation induces an opposite effect on alloreactive CD4(+) and CD8(+) T cells in graft-versus-host disease. *J Exp Med* **200**(2):149-157.
- Nocentini G, Cuzzocrea S, Bianchini R, Mazzon E and Riccardi C (2007a) Modulation of acute and chronic inflammation of the lung by GITR and its ligand. *Ann N Y Acad Sci* **1107**:380-391.
- Nocentini G, Giunchi L, Ronchetti S, Krausz LT, Bartoli A, Moraca R, Migliorati G and Riccardi C (1997) A new member of the tumor necrosis factor/nerve growth factor receptor family inhibits T cell receptor-induced apoptosis. *Proc Natl Acad Sci U S A* **94**(12):6216-6221.

- Nocentini G and Riccardi C (2005) GITR: a multifaceted regulator of immunity belonging to the tumor necrosis factor receptor superfamily. *Eur J Immunol* **35**(4):1016-1022.
- Nocentini G, Ronchetti S, Cuzzocrea S and Riccardi C (2007b) GITR/GITRL: More than an effector T cell co-stimulatory system. *Eur J Immunol* **37**(5):1165-1169.
- Patel M, Xu D, Kewin P, Choo-Kang B, McSharry C, Thomson NC and Liew FY (2005) Glucocorticoid-induced TNFR family-related protein (GITR) activation exacerbates murine asthma and collagen-induced arthritis. *Eur J Immunol* **35**(12):3581-3590.
- Ramirez-Montagut T, Chow A, Hirschhorn-Cymerman D, Terwey TH, Kochman AA, Lu S, Miles RC, Sakaguchi S, Houghton AN and van den Brink MR (2006) Glucocorticoid-Induced TNF Receptor Family Related Gene Activation Overcomes Tolerance/Ignorance to Melanoma Differentiation Antigens and Enhances Antitumor Immunity. *J Immunol* **176**(11):6434-6442.
- Ronchetti S, Nocentini G, Bianchini R, Krausz LT, Migliorati G and Riccardi C (2007) GITR lowers the threshold of CD28 costimulation in CD8+ T cells. *J Immunol* **179**:5916-5926.
- Ronchetti S, Nocentini G, Riccardi C and Pandolfi PP (2002) Role of GITR in activation response of T lymphocytes. *Blood* **100**(1):350-352.
- Ronchetti S, Zollo O, Bruscoli S, Agostini M, Bianchini R, Nocentini G, Ayroldi E and Riccardi C (2004) GITR, a member of the TNF receptor superfamily, is costimulatory to mouse T lymphocyte subpopulations. *Eur J Immunol* **34**(3):613-622.
- Sakamoto A, Ohnishi ST, Ohnishi T and Ogawa R (1991) Relationship between free radical production and lipid peroxidation during ischemia-reperfusion injury in the rat brain. *Brain Res* **554**(1-2):186-192.
- Seki T, Hida K, Tada M, Koyanagi I and Iwasaki Y (2003) Role of the bcl-2 gene after contusive spinal cord injury in mice. *Neurosurgery* **53**(1):192-198.
- Shea TB (1994) Technical report. An inexpensive densitometric analysis system using a Macintosh computer and a desktop scanner. *BioTechniques* **16**(6):1126-1128.

- Shin HH, Kim SJ, Lee DS and Choi HS (2005) Soluble glucocorticoid-induced tumor necrosis factor receptor (sGITR) stimulates osteoclast differentiation in response to receptor activator of NF-kappaB ligand (RANKL) in osteoclast cells. *Bone* **36**(5):832-839.
- Shin HH, Lee HW and Choi HS (2003) Induction of nitric oxide synthase (NOS) by soluble glucocorticoid induced tumor necrosis factor receptor (sGITR) is modulated by IFN-gamma in murine macrophage. *Exp Mol Med* **35**(3):175-180.
- Sirin BH, Ortac R, Cerrahoglu M, Saribulbul O, Baltalarli A, Celebisoy N, Iskesen I and Rendeci O (2002) Ischaemic preconditioning reduces spinal cord injury in transient ischaemia. *Acta cardiologica* **57**(4):279-285.
- Tone M, Tone Y, Adams E, Yates SF, Frewin MR, Cobbold SP and Waldmann H (2003) Mouse glucocorticoid-induced tumor necrosis factor receptor ligand is costimulatory for T cells. *Proc Natl Acad Sci U S A* **100**(25):15059-15064.

FOOTNOTES

This study was supported by Associazione Italiana Ricerca sul Cancro (Milan, Italy) and by the network FIRB Grant, protocol RBPR05NWWC "CHEM-PROFARMA-NET" (Italy).

¹These authors contributed equally to this work.

FIGURE LEGENDS

Figure 1. Higher motor score in SCI-GITR^{-/-} as compared to SCI-GITR^{+/+} mice following SCI. Mice were observed for 10 day following SCI (panel b) and sham treatment (panel a). Difference between SCI-GITR^{-/-} and SCI-GITR^{+/+} mice began to be significant 4 days after SCI (*, p<0.05 and **, p<0.01)

Figure 2. Reduced spinal cord injury in SCI-GITR^{-/-} and SCI-GITR^{+/+} mice treated with GITR-Fc as compared to SCI-GITR^{+/+} mice. Spinal cord sections from a sham-operated GITR^{+/+} (a) and GITR^{-/-} mice (b), 24 hours after trauma, are shown. A spinal cord section of SCI-GITR^{+/+} mice including white (wm) and gray (gm) matters shows edema and alteration of the wm (c), that were reduced in SCI-GITR^{-/-} mice (d). To show the lesions in SCI-GITR^{+/+} mice, a higher magnification is also shown (panel c1). A spinal cord section of SCI-GITR^{+/+} mice treated with GITR-Fc, demonstrating reduced lesions, is shown in panel e. Sections of SCI-GITR^{+/+} mice treated with control Fc are similar to untreated SCI-GITR^{+/+} mice (not shown). A spinal cord section of SCI-GITR^{-/-} mice treated with GITR-Fc, demonstrating lesions similar to SCI-GITR^{-/-}, is also shown (f). Figures are representative of three experiments performed on different experimental days (5 mice/group). Histological score derived from all the experiments are also reported (g). The histological scores of SCI-mice were compared with the respective sham-mice and significance is reported (***, p<0.001; *, p<0.05). The histological score of SCI-GITR^{-/-} mice and of GITR-Fc-treated SCI-GITR^{+/+} mice is significantly different from that of untreated SCI-GITR^{+/+} mice (++, p<0.01), but the histological score of Fc-treated SCI-GITR^{+/+} is not significantly different from that of untreated SCI-GITR^{+/+} mice (n.s., p>0.05) and the histological score of GITR-Fc-treated SCI-GITR^{-/-} mice is not significantly different from that of untreated SCI-GITR^{-/-} mice (n.s., p>0.05).

Figure 3. Reduced loss of myelin structure in SCI-GITR^{-/-} and SCI-GITR^{+/-} mice treated with GITR-Fc as compared to SCI-GITR^{+/+} mice. Spinal cord sections including white (wm) and gray (gm) matters, stained with Luxol fast blue, from a sham-operated GITR^{+/+} (a) and GITR^{-/-} mice (b), 24 hours after SCI, are shown. A spinal cord section of SCI-GITR^{+/+} mice shows loss of myelin (c), that is less evident in SCI-GITR^{-/-} mice (d). A spinal cord section of SCI-GITR^{+/-} (e) and SCI-GITR^{-/-} (f) mice treated with GITR-Fc, demonstrating loss of myelin similar to that observed in SCI-GITR^{-/-} mice, is also shown. Figures are representative of three experiments performed on different experimental days (5 mice/group).

Figure 4. Lower expression of nitrotyrosine in the spinal cord of SCI-GITR^{-/-} and SCI-GITR^{+/-} mice treated with GITR-Fc as compared to SCI-GITR^{+/+} mice. Immunohistochemical staining of spinal cord sections from sham-operated mice with anti-nitrotyrosine antibody are negative (panel a and b). A spinal cord section, including white (wm) and gray (gm) matters, of SCI-GITR^{+/+} mice shows nitrotyrosine staining (panel c). Staining was less in SCI-GITR^{-/-} mice (panel d) and in SCI-GITR^{+/-} mice treated with GITR-Fc (panel e). Nitrotyrosine staining seen in SCI-GITR^{+/+} mice treated with control Fc is similar to that observed in untreated SCI-GITR^{+/+} mice (not shown) and staining seen in SCI-GITR^{-/-} mice treated with GITR-Fc (panel f) is similar to that observed in untreated SCI-GITR^{-/-} mice. Figures are representative of three experiments performed on different experimental days. To quantify the presence of nitrotyrosine, the area stained with anti-nitrotyrosine antibody was calculated and the mean of all experiments was reported for all groups (panel g). The levels of nitrotyrosine staining in SCI-mice were compared with the respective sham-mice and significance is reported (***, p<0.001; *, p<0.05). Nitrotyrosine staining in SCI-GITR^{-/-} mice and in GITR-Fc-treated SCI-GITR^{+/+} mice is significantly less than that of untreated SCI-GITR^{+/+} mice (++, p<0.01). Nitrotyrosine staining of Fc-treated SCI-GITR^{+/+} is not significantly different from that of untreated SCI-GITR^{+/+} mice (n.s., p>0.05) and that of GITR-Fc-treated SCI-GITR^{-/-} mice is not significantly different from that of untreated SCI-GITR^{-/-} mice (n.s., p>0.05).

Figure 5. Lower expression of iNOS in the spinal cord of SCI-GITR^{-/-} and SCI-GITR^{+/+} mice treated with GITR-Fc as compared to SCI-GITR^{+/+} mice. Immunohistochemical staining of spinal cord sections from sham-operated mice with anti-iNOS antibody is negative (panel a and b). A spinal cord section, including white (wm) and gray (gm) matters, of SCI-GITR^{+/+} mice shows iNOS staining (panel c). Staining was less in SCI-GITR^{-/-} mice (panel d) and in SCI-GITR^{+/+} mice treated with GITR-Fc (panel e). iNOS staining seen in SCI-GITR^{+/+} mice treated with control Fc is similar to that observed in untreated SCI-GITR^{+/+} mice (not shown) and staining seen in SCI-GITR^{-/-} mice treated with GITR-Fc is similar to that observed in untreated SCI-GITR^{-/-} mice (panel f). Figures are representative of three experiments performed on different experimental days (5 mice/group). To quantify the presence of iNOS, the area stained with anti-iNOS antibody was calculated and the mean of all experiments was reported for all groups (panel g). The levels of iNOS staining in SCI-mice were compared with the respective sham-mice and significance is reported (***, p<0.001; *, p<0.05). iNOS staining in SCI-GITR^{-/-} mice and in GITR-Fc-treated SCI-GITR^{+/+} mice is significantly less than that of untreated SCI-GITR^{+/+} mice (++, p<0.01). iNOS staining of Fc-treated SCI-GITR^{+/+} is not significantly different from that of untreated SCI-GITR^{+/+} mice (n.s., p>0.05) and that of GITR-Fc-treated SCI-GITR^{-/-} mice is not significantly different from that of untreated SCI-GITR^{-/-} mice (n.s., p>0.05).

Figure 6. Lower production of IL-2 cytokine in the spinal cord of SCI-GITR^{-/-} and SCI-GITR^{+/+} mice treated with GITR-Fc as compared to SCI-GITR^{+/+} mice. Immunohistochemical staining of spinal cord from sham-operated mice with anti-IL-2 antibody were negative (panels a and b). A spinal cord section of SCI-GITR^{+/+} mice, including white (wm) and gray (gm) matters, shows IL-2 staining (panel c). Staining was less in SCI-GITR^{-/-} mice (panel d) and in SCI-GITR^{+/+} mice treated with GITR-Fc (panel e). IL-2 staining seen in GITR^{+/+} mice treated with control Fc is similar to that observed in untreated SCI-GITR^{+/+} mice (not shown) and staining seen in SCI-GITR^{-/-} mice treated

with GITR-Fc is similar to that observed in untreated SCI-GITR^{-/-} mice (panel f). Figures are representative of three experiments performed on different experimental days (5 mice/groups). To quantify the presence of IL-2, the area stained with anti-IL-2 antibody was calculated and the mean of all experiments was reported for all groups (panel g). The levels of IL-2 in SCI-mice were compared with the respective sham-mice and significance is reported (***, p<0.001; *, p<0.05). IL-2 in SCI-GITR^{-/-} mice and in GITR-Fc-treated SCI-GITR^{+/+} mice is significantly less than that of untreated SCI-GITR^{+/+} mice (***, p<0.001). IL-2 staining of Fc-treated SCI-GITR^{+/+} is not significantly different from that of untreated SCI-GITR^{+/+} mice (n.s., p>0.05) and that of GITR-Fc-treated SCI-GITR^{-/-} mice is not significantly different from that of untreated SCI-GITR^{-/-} mice (n.s., p>0.05).

Figure 7. Lower production of IL-12 and TNF- α in the spinal cord of SCI-GITR^{-/-} and SCI-GITR^{+/+} mice treated with GITR-Fc as compared to SCI-GITR^{+/+} mice. Immunohistochemical staining of spinal cord from the different groups is shown in Figures s1 and s2 of the supplementary material. To quantify the presence of IL-12 and TNF- α , the area stained with antibodies was calculated and the mean of all experiments was reported for all groups (panel a and b, respectively). The levels of IL-12 and TNF- α in SCI-mice were compared with the respective sham-mice and significance is reported (***, p<0.001; *, p<0.05). IL-12 and TNF- α levels in SCI-GITR^{-/-} mice and in GITR-Fc-treated SCI-GITR^{+/+} mice were significantly less than that of untreated SCI-GITR^{+/+} mice (++, p<0.01). Staining of Fc-treated SCI-GITR^{+/+} were not significantly different from that of untreated SCI-GITR^{+/+} mice (n.s., p>0.05) and that of GITR-Fc-treated SCI-GITR^{-/-} mice were not significantly different from that of untreated SCI-GITR^{-/-} mice (n.s., p>0.05).

Figure 8. The decreased proliferation of anti-CD3 activated T lymphocytes following GITR-Fc treatment is observed in cells from GITR^{+/+} mice and not from GITR^{-/-} mice. CFSE labeled cells from lymph nodes of GITR^{+/+} (panel a) and GITR^{-/-} (panel b) mice were activated with anti-CD3 (1

or 0.5 $\mu\text{g/ml}$, respectively) and co-treated with Fc control protein (left) or GITR-Fc fusion protein (right). After 72 h treatment, flow cytometric analysis of CFSE was performed and 1 representative experiment is shown. The percentage of cells undergoing at least 1 cell cycle is also reported. Panel c shows the increase or decrease in the percentage of cycling T cells from spleen and lymph nodes, activated with the specified anti-CD3 concentrations. Results are the mean of four experiments and in each experiment the cells derives from a pool of 4 mice. The significance of the difference of proliferating cells in GITR-Fc co-treated vs Fc co-treated cells is also reported (**, $p < 0.01$; *, $p < 0.05$; n.s., $p > 0.05$).

Figure 9. Lower apoptosis and apoptosis-related markers in the spinal cord of SCI-GITR^{-/-} and SCI-GITR^{+/+} mice treated with GITR-Fc as compared to SCI-GITR^{+/+} mice. Apoptosis was evaluated through TUNEL staining of spinal cord and is shown in Figure s3 of supplemental material. The number of TUNEL positive cells in the different groups was evaluated and reported in panel a. Apoptosis levels in SCI-mice were compared with those of the respective sham-mice and significance is reported (***, $p < 0.001$; *, $p < 0.05$). Apoptosis levels in SCI-GITR^{-/-} mice and in GITR-Fc-treated SCI-GITR^{+/+} mice were significantly less than that of untreated SCI-GITR^{+/+} mice (++, $p < 0.01$). Apoptosis in Fc-treated SCI-GITR^{+/+} sections was not significantly different from that of untreated SCI-GITR^{+/+} mice (n.s., $p > 0.05$) and that of GITR-Fc-treated SCI-GITR^{-/-} mice were not significantly different from that of untreated SCI-GITR^{-/-} mice (n.s., $p > 0.05$). Immunohistochemical staining of spinal cord with anti-FasL, anti-Bax and anti-Bcl-2 is shown in Figures s4, s5 and s6 of supplemental material. To quantify the presence of FasL, Bax and Bcl-2, the area stained with antibodies was calculated and the mean of all experiments was reported for all groups (panel b, c and d, respectively). The levels of FasL, Bax and Bcl-2 in SCI-mice were compared with those of the respective sham-mice and significance is reported (***, $p < 0.001$; *, $p < 0.05$). FasL and Bax levels in SCI-GITR^{-/-} mice and in GITR-Fc-treated SCI-GITR^{+/+} mice were significantly less than that of untreated SCI-GITR^{+/+} mice (++, $p < 0.01$). Staining of Fc-treated SCI-

GITR^{+/+} were not significantly different from that of untreated SCI-GITR^{+/+} mice (n.s., p>0.05) and that of GITR-Fc-treated SCI-GITR^{-/-} mice were not significantly different from that of untreated SCI-GITR^{-/-} mice (n.s., p>0.05). Bcl-2 levels in SCI-GITR^{-/-} mice and in GITR-Fc-treated SCI-GITR^{+/+} mice were significantly more than that of untreated SCI-GITR^{+/+} mice (++, p<0.01). Staining of Fc-treated SCI-GITR^{+/+} were not significantly different from that of untreated SCI-GITR^{+/+} mice (n.s., p>0.05) and that of GITR-Fc-treated SCI-GITR^{-/-} mice were not significantly different from that of untreated SCI-GITR^{-/-} mice (n.s., p>0.05).

Figure 10. Lower CD4⁺ T lymphocyte infiltration in the spinal cord of SCI-GITR^{-/-} and SCI-GITR^{+/+} mice treated with GITR-Fc as compared to SCI-GITR^{+/+} mice. Spinal cord sections from sham-operated mice did not show CD4⁺ cell infiltration, as expected (panels a and b). A spinal cord section of SCI-GITR^{+/+} mice including white (wm) and gray (gm) matters shows CD4⁺ T cell infiltration (panel c). T lymphocytes are indicated by arrows in panel c1 showing a section at a higher magnification. CD4⁺ T cell infiltration was less in SCI-GITR^{-/-} mice (panel d) and in SCI-GITR^{+/+} mice treated with GITR-Fc (panel e). T cell infiltration seen in GITR^{+/+} mice treated with control Fc are similar to that observed in untreated SCI-GITR^{+/+} mice (not shown) and staining seen in SCI-GITR^{-/-} mice treated with GITR-Fc is similar to that observed in untreated SCI-GITR^{-/-} mice (panel f). Figures are representative of three experiments performed on different experimental days (5 mice/group). To quantify T cell infiltration, the area stained with anti-CD4 antibody was calculated and the mean of all experiments was reported for all groups (panel g). The levels of T cell infiltration of SCI-mice were compared with the respective sham-mice and significance is reported (***, p<0.001; *, p<0.05). Infiltration of spinal cord sections in SCI-GITR^{-/-} mice and GITR-Fc-treated SCI-GITR^{+/+} mice is significantly less from that of untreated SCI-GITR^{+/+} mice (++, p<0.01). Infiltration of spinal cord sections in Fc-treated SCI-GITR^{+/+} is not significantly different from that of untreated SCI-GITR^{+/+} mice (n.s., p>0.05) and that of GITR-Fc-treated SCI-GITR^{-/-} mice is not significantly different from that of untreated SCI-GITR^{-/-} mice (n.s., p>0.05).

Figure 11. Lower CD8⁺ T lymphocyte infiltration in the spinal cord of SCI-GITR^{-/-} mice and SCI-GITR^{+/+} mice treated with GITR-Fc as compared to SCI-GITR^{+/+} mice. Spinal cord sections from sham-operated mice did not show CD8⁺ cell infiltration (panels a and b). A spinal cord section of SCI-GITR^{+/+} mice including white (wm) and gray (gm) matters shows CD8⁺ T cell infiltration (panel c). T lymphocytes are indicated by arrows, in panel 1c showing sections at a higher magnification. CD8⁺ T cell infiltration was less in SCI-GITR^{-/-} mice (panel d) and in SCI-GITR^{+/+} mice treated with GITR-Fc (panel e). T cell infiltration seen in GITR^{+/+} mice treated with control Fc are similar to that observed in untreated SCI-GITR^{+/+} mice (not shown) and staining seen in SCI-GITR^{-/-} mice treated with GITR-Fc is similar to that observed in untreated SCI-GITR^{-/-} mice (panel f). Figures are representative of three experiments performed on different experimental days (5 mice/group). To quantify T cell infiltration, the area stained with anti-CD8 antibody was calculated and the mean of all experiments was reported for all groups (panel g). The levels of T cell infiltration of SCI-mice were compared with the respective sham-mice and significance is reported (***, p<0.001; *, p<0.05). Infiltration of spinal cord sections in SCI-GITR^{-/-} mice and GITR-Fc-treated SCI-GITR^{+/+} mice is significantly less from that of untreated SCI-GITR^{+/+} mice (++, p<0.01). Infiltration of spinal cord sections in Fc-treated SCI-GITR^{+/+} is not significantly different from that of untreated SCI-GITR^{+/+} mice (n.s., p>0.05) and that of GITR-Fc-treated SCI-GITR^{-/-} mice is not significantly different from that of untreated SCI-GITR^{-/-} mice (n.s., p>0.05).

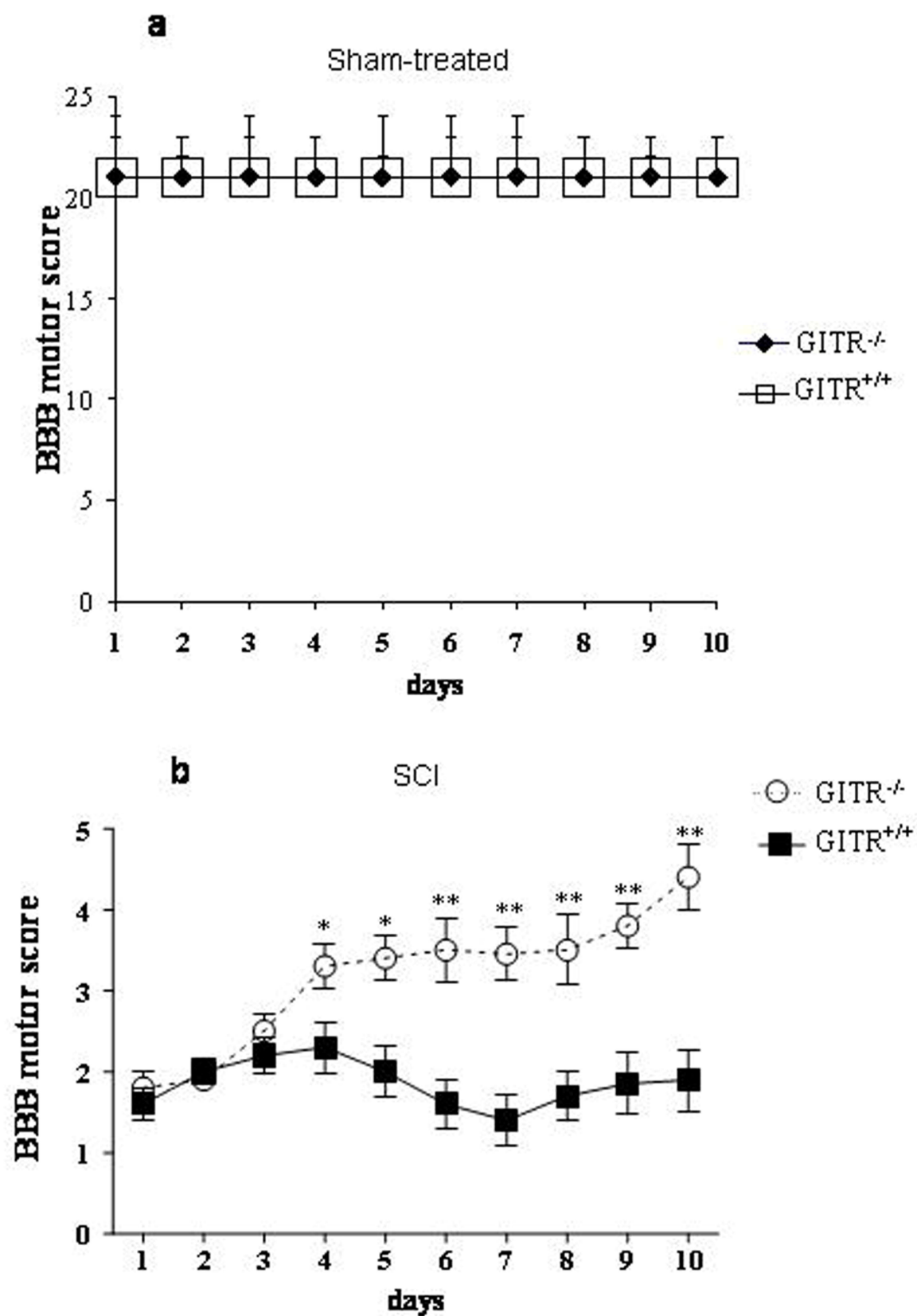


FIG.1

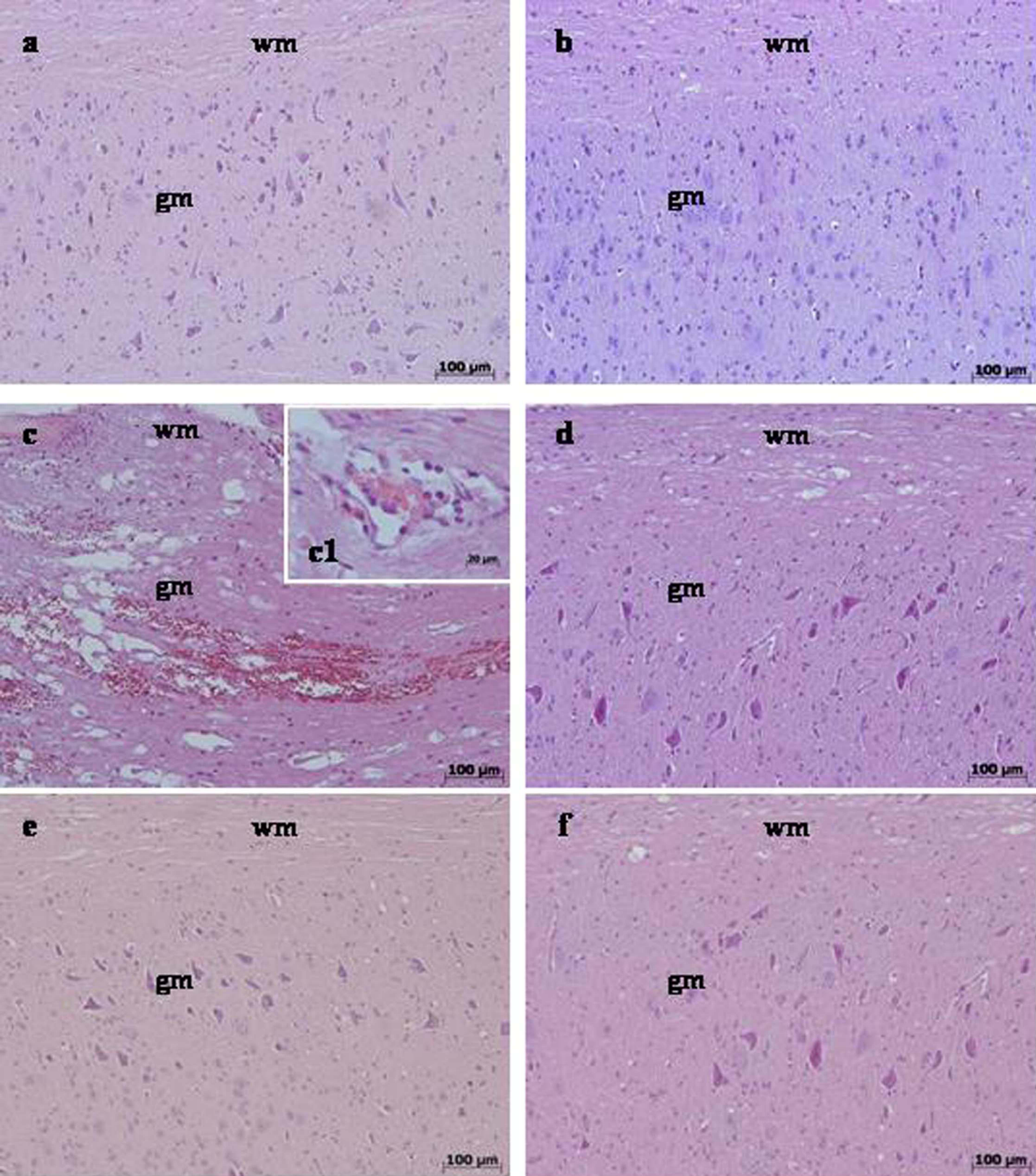


FIG.2

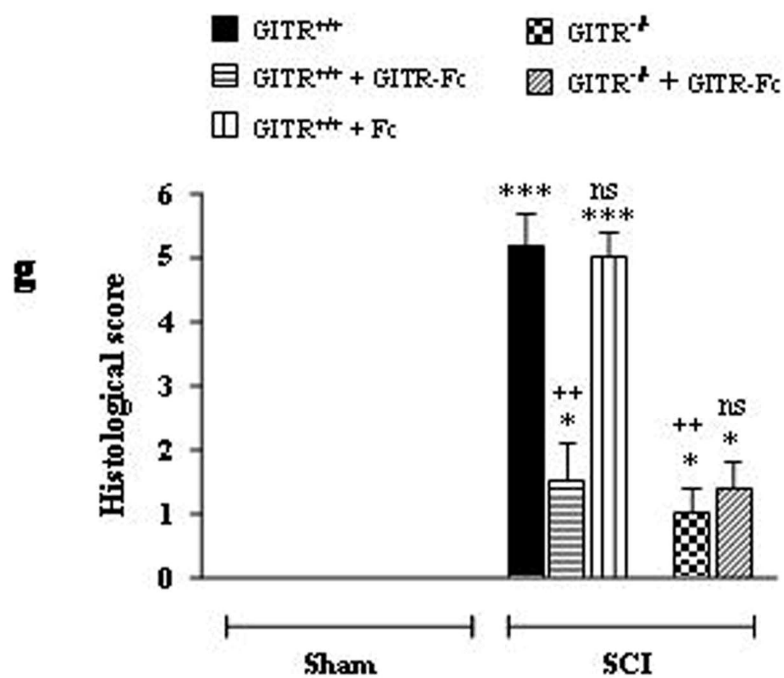


FIG.2

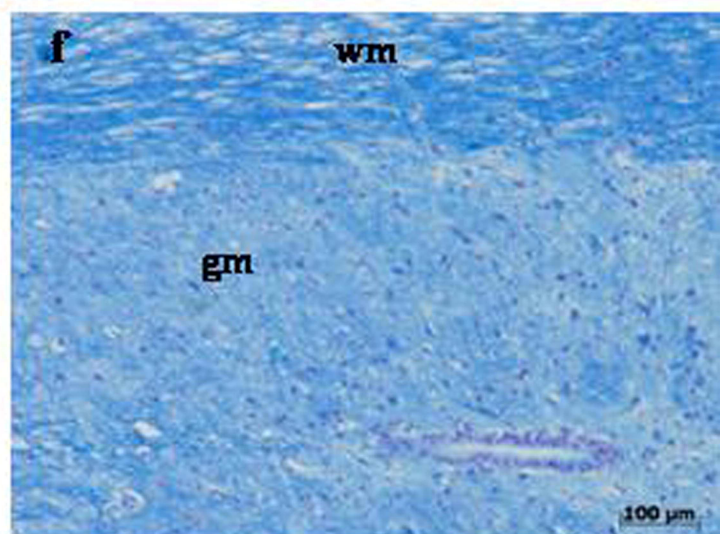
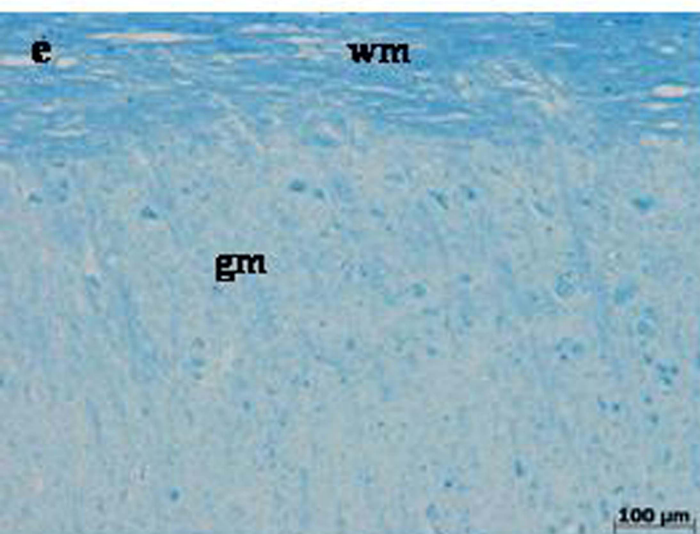
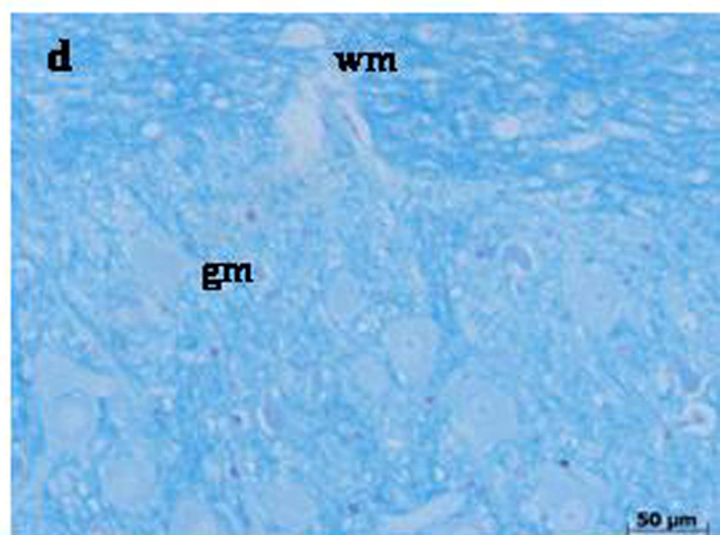
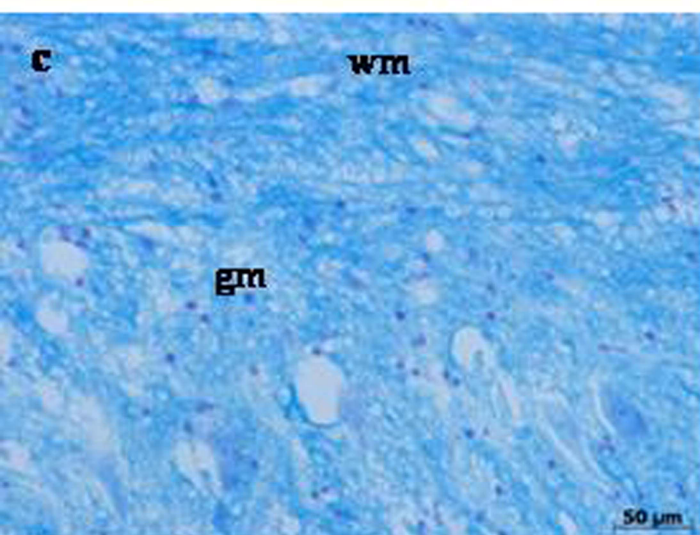
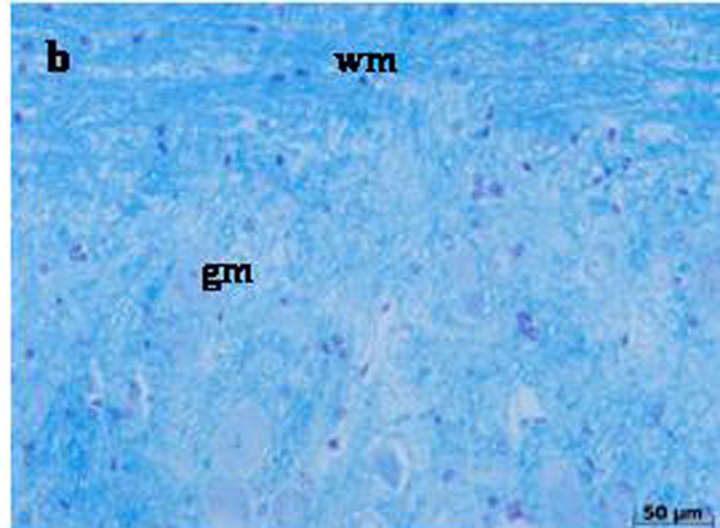
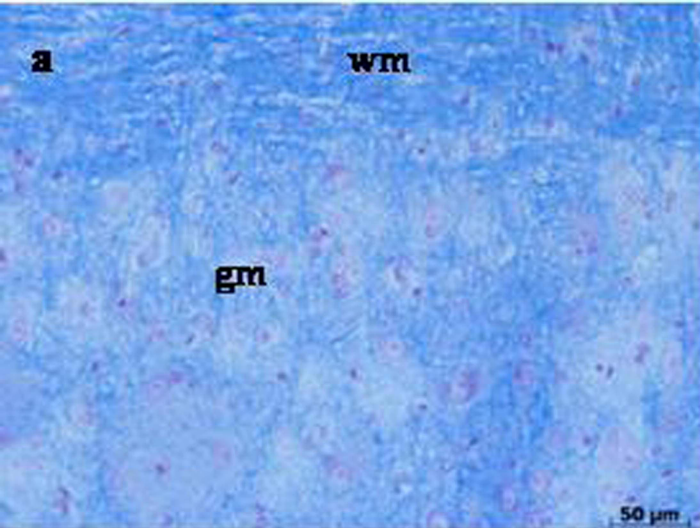


FIG.3

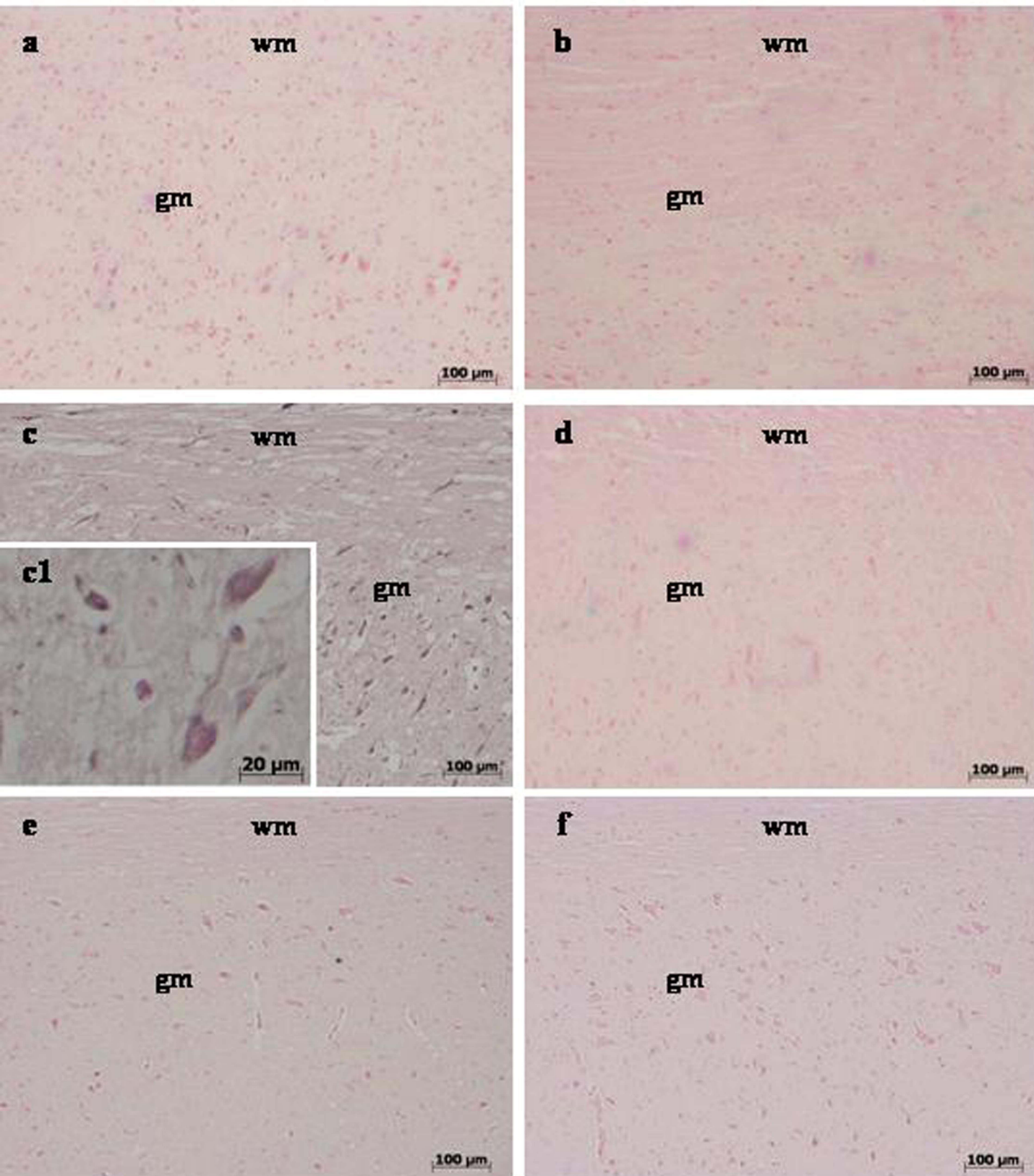


FIG.4

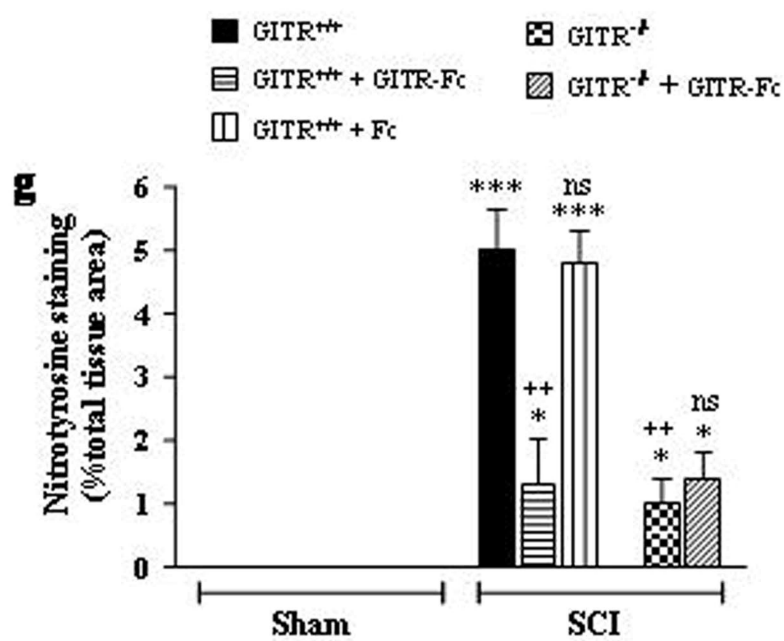


FIG.4

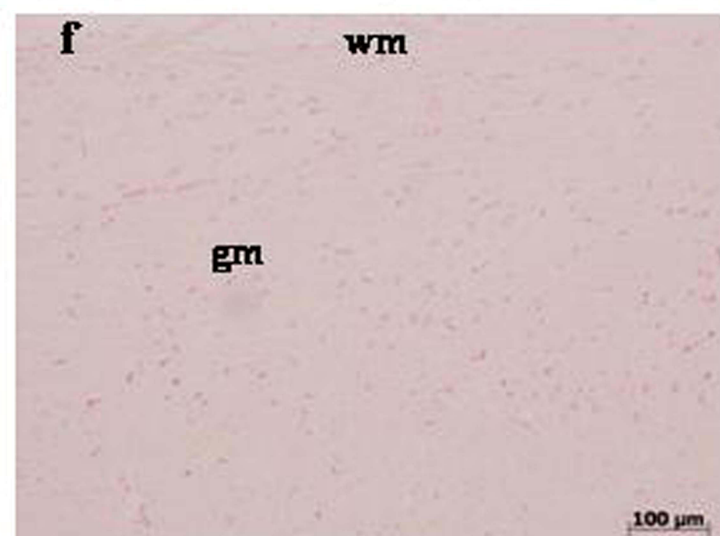
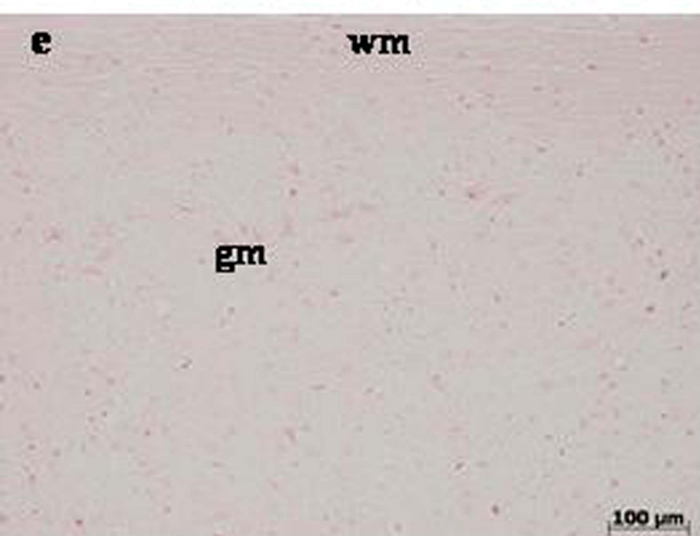
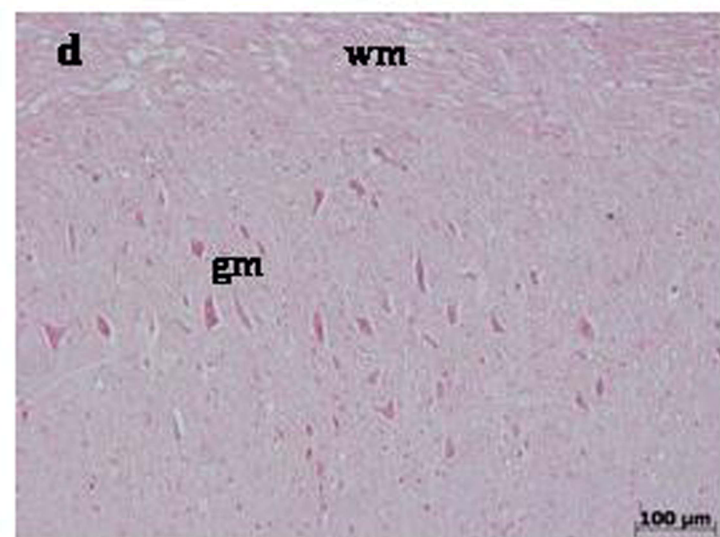
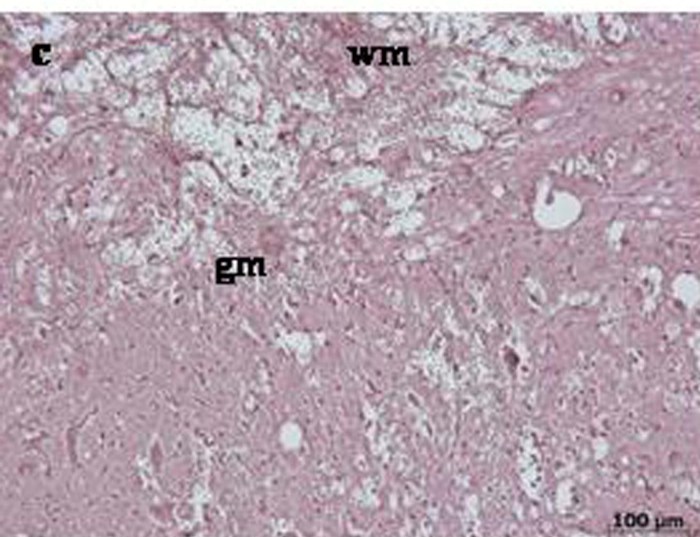
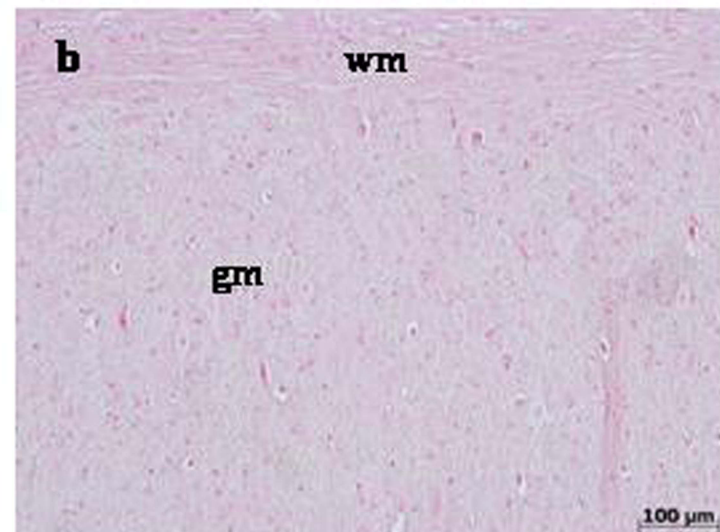
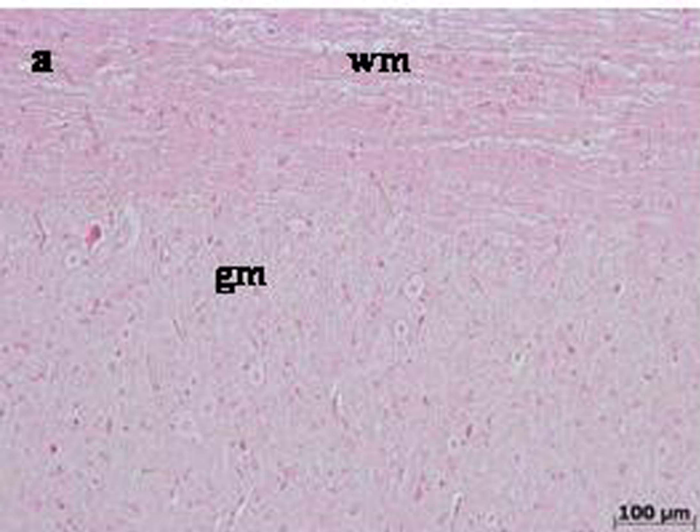


FIG. 5

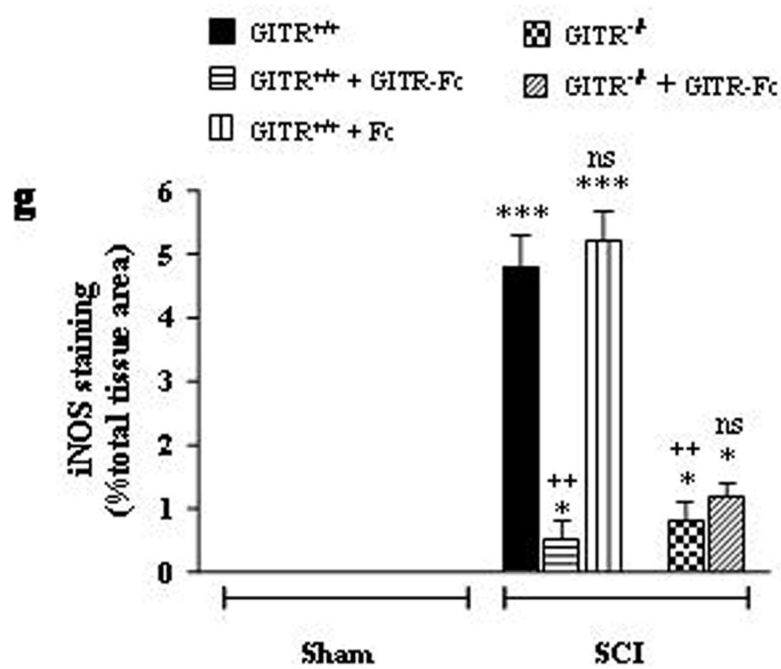


FIG. 5

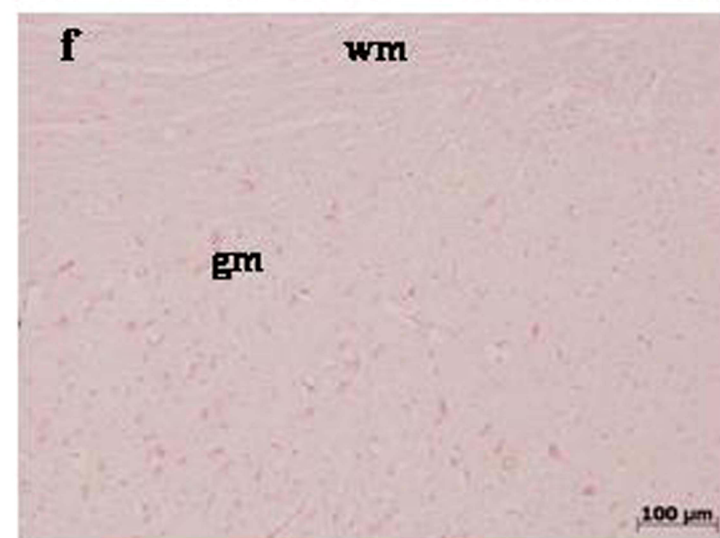
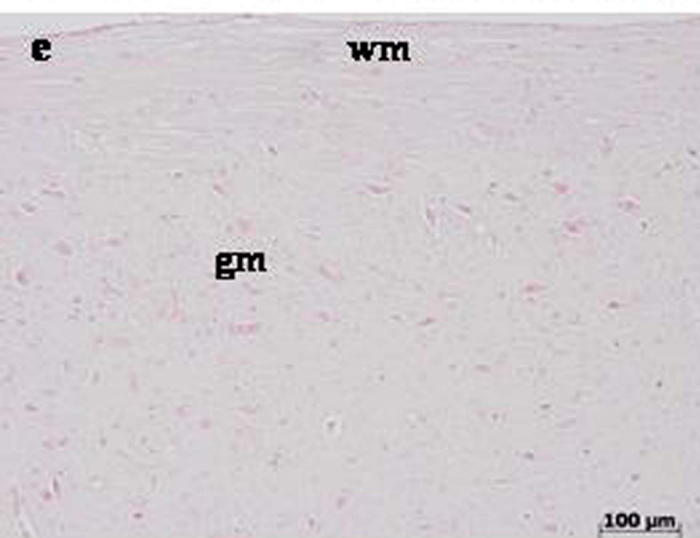
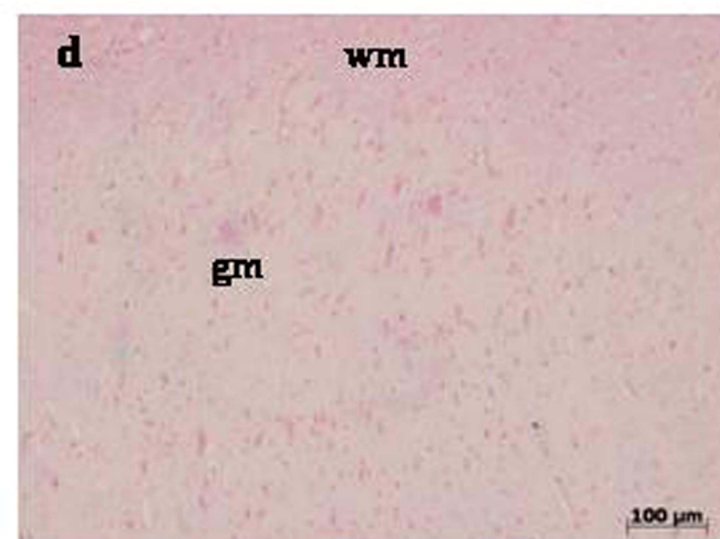
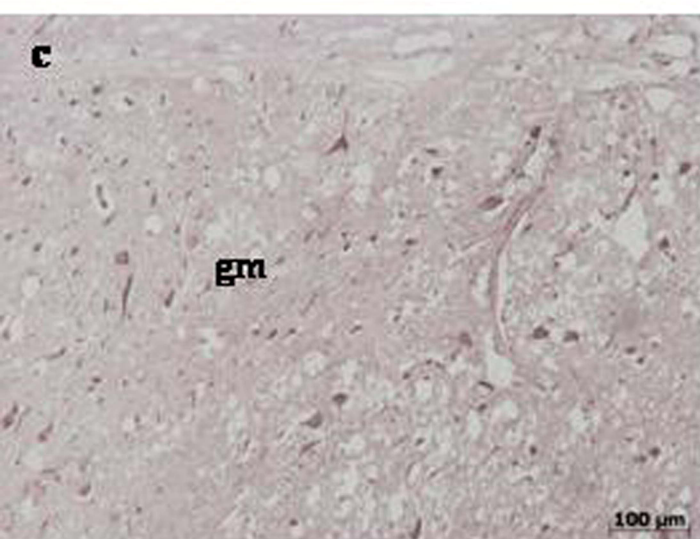
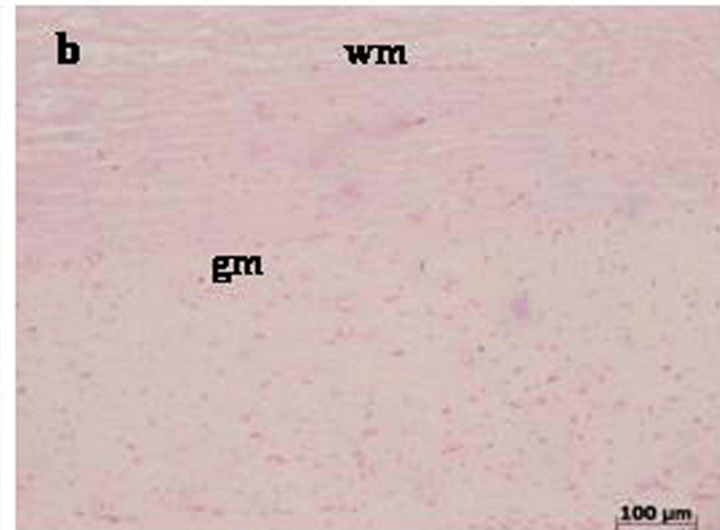
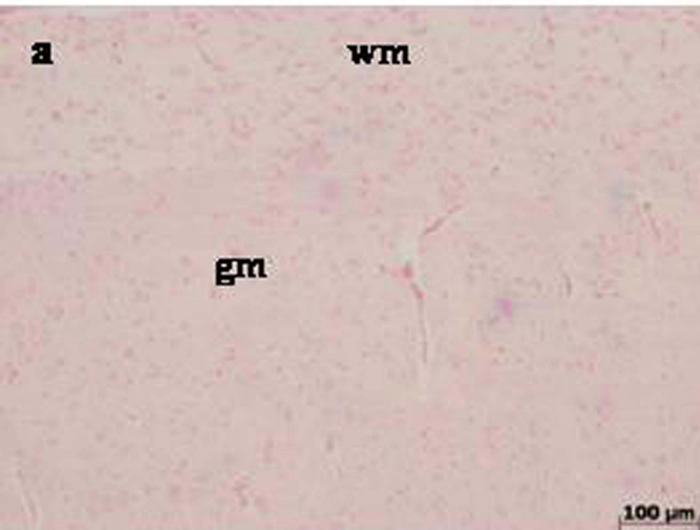


FIG.6

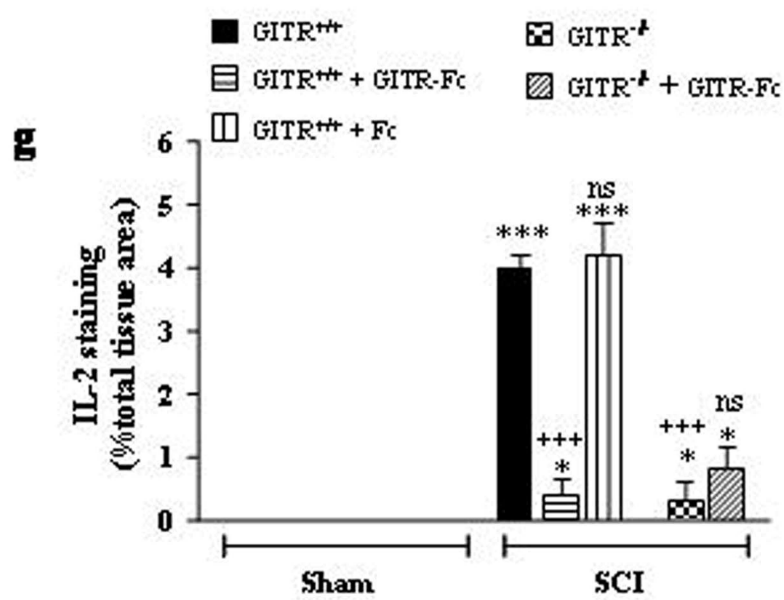


FIG.6

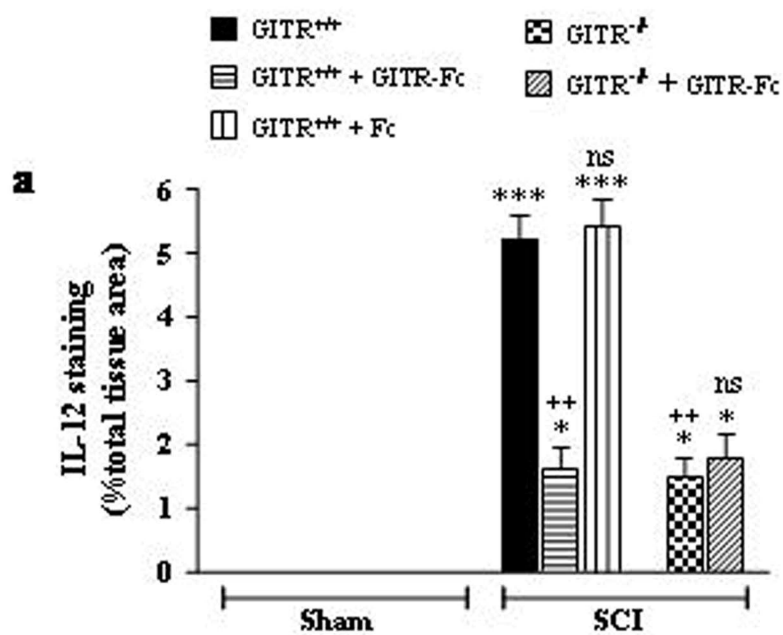


FIG.7

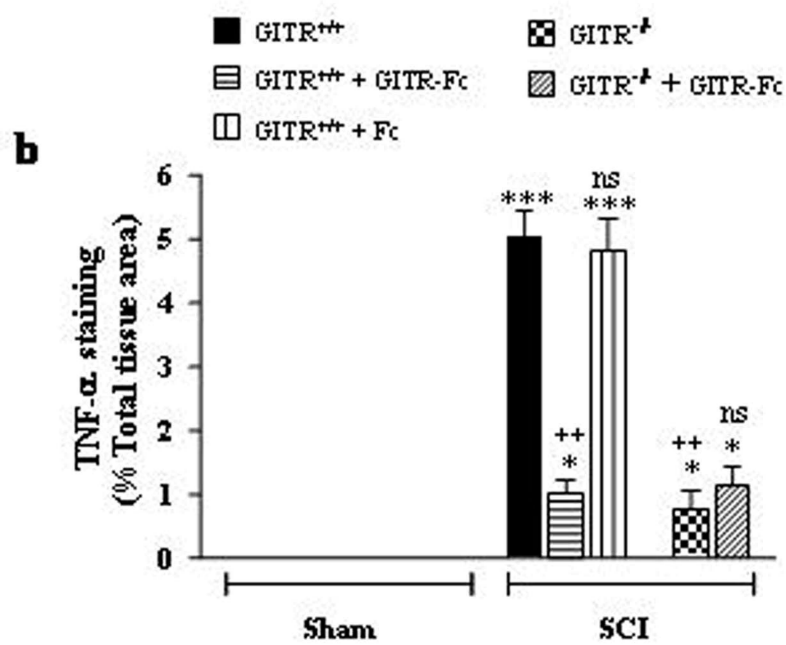


FIG.7

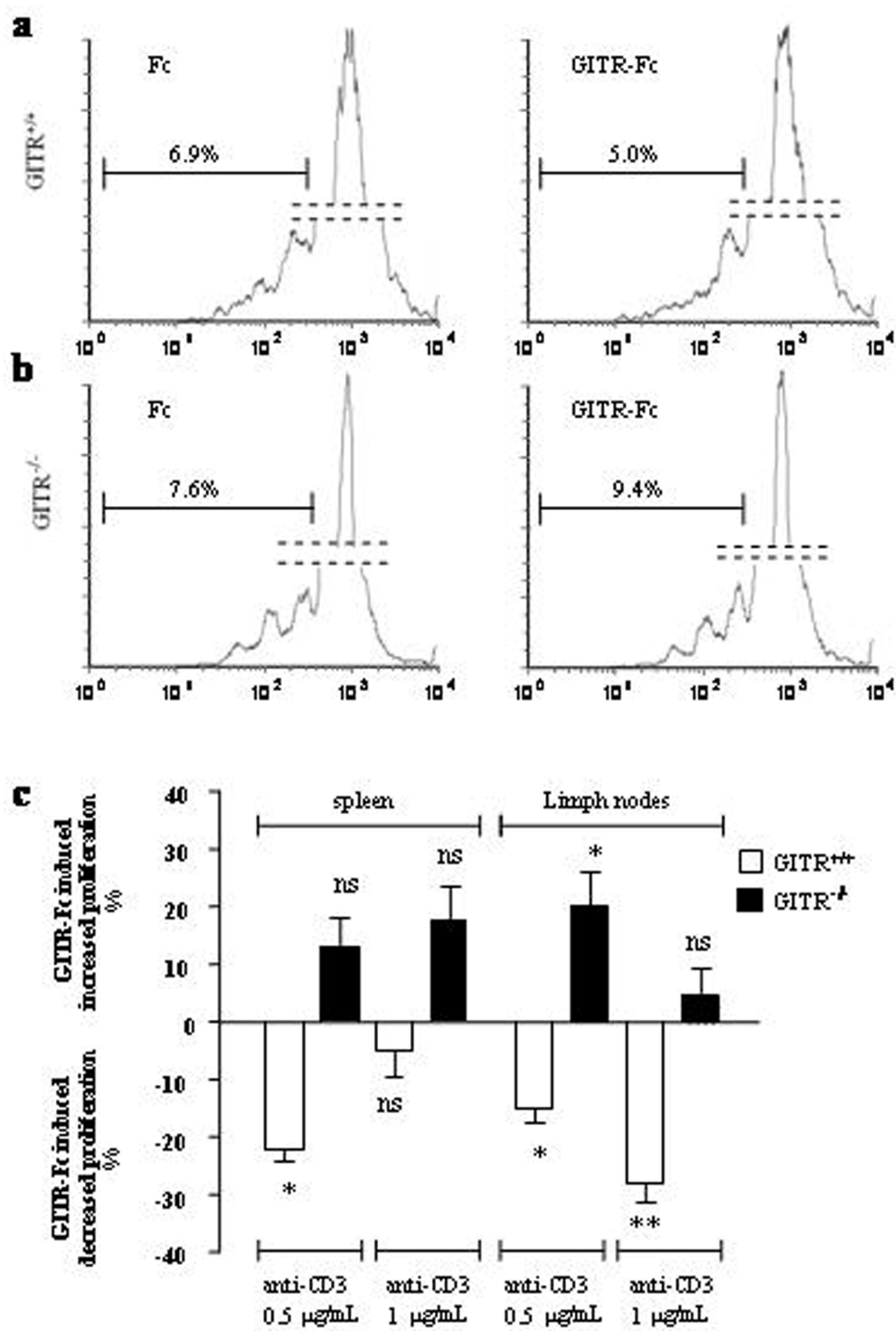


FIG. 8

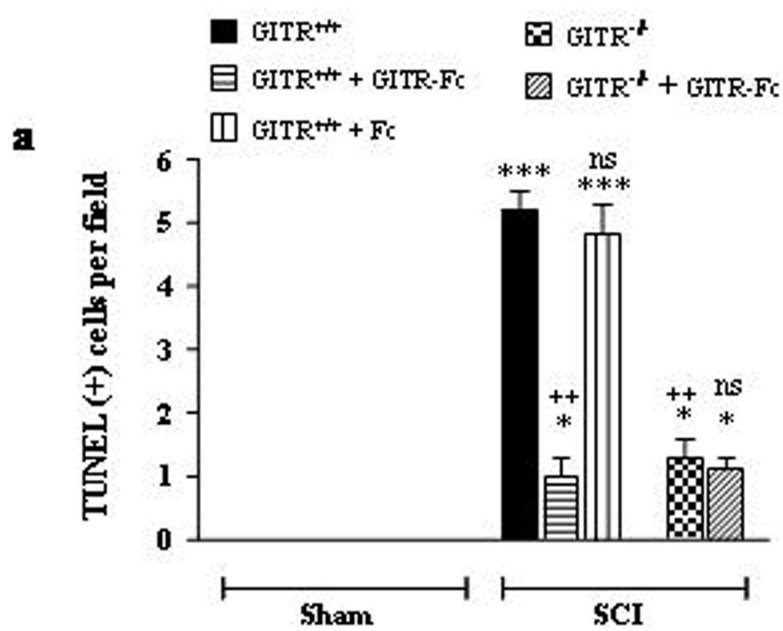


FIG.9

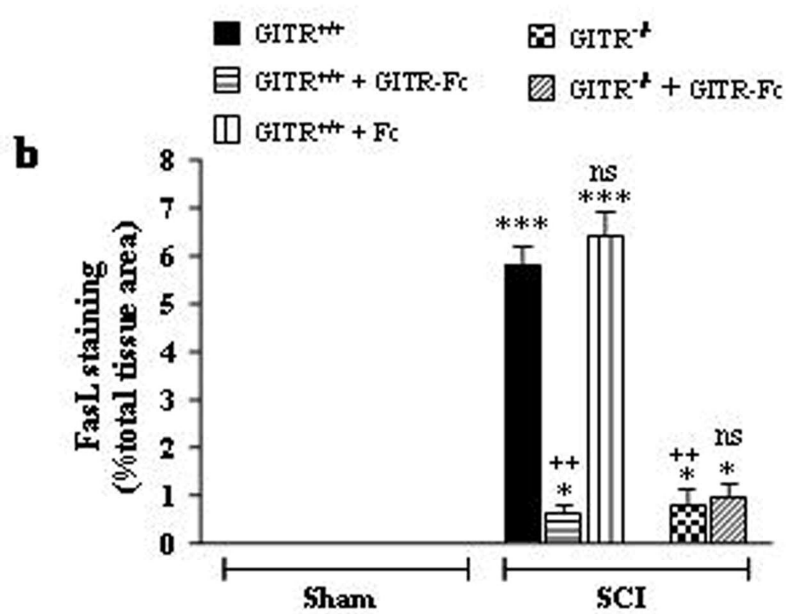


FIG.9

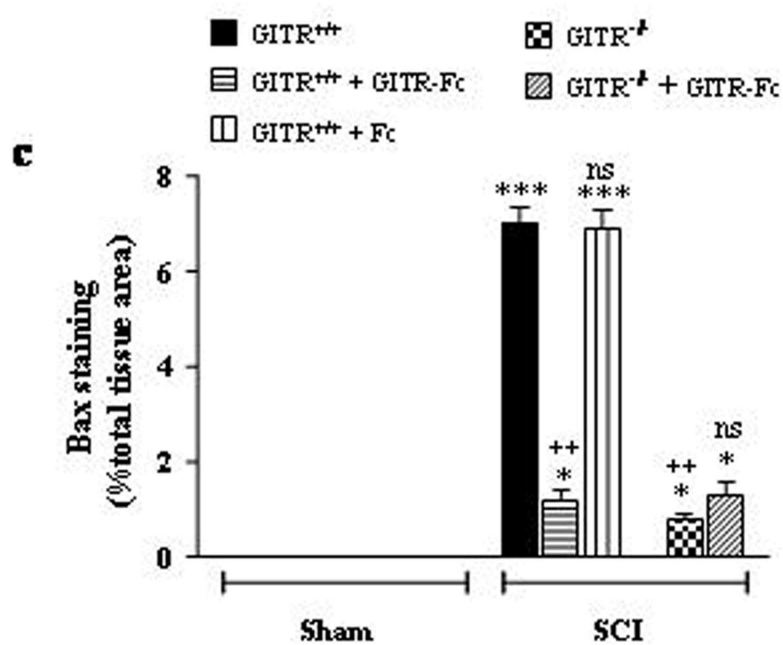


FIG.9

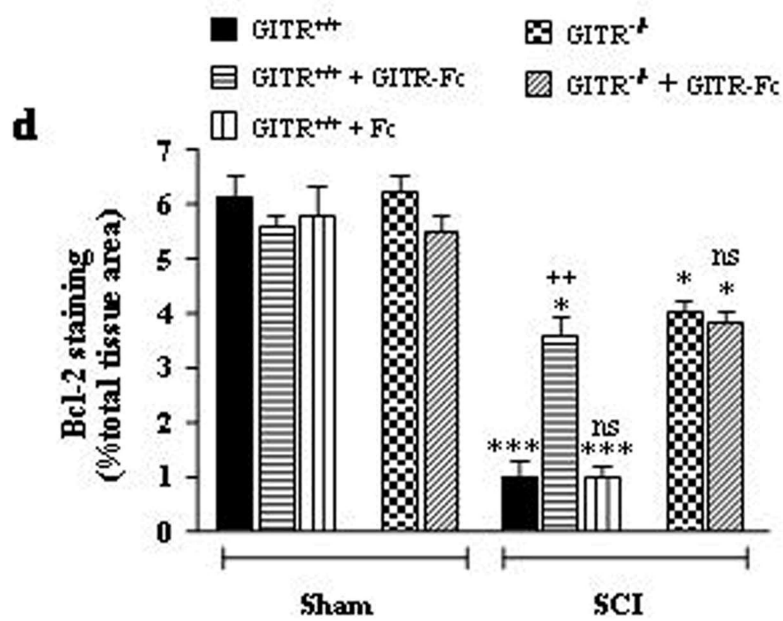


FIG.9

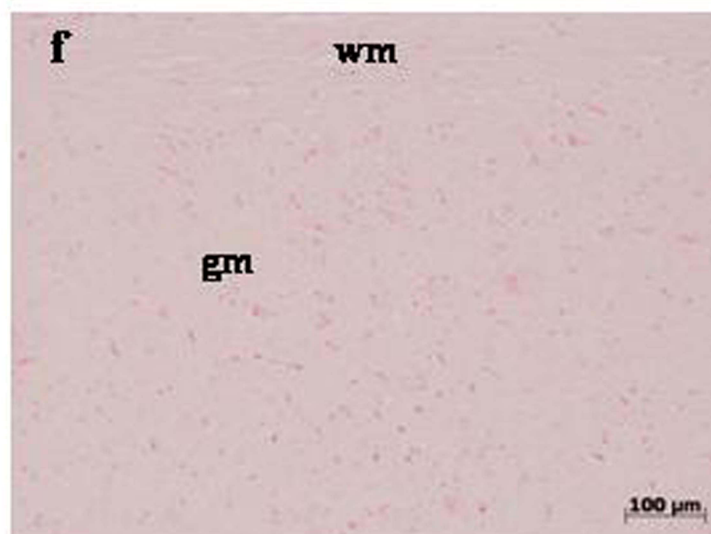
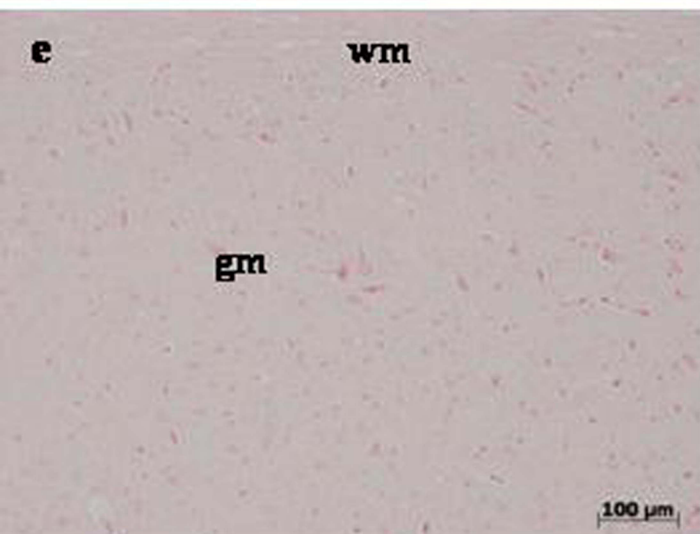
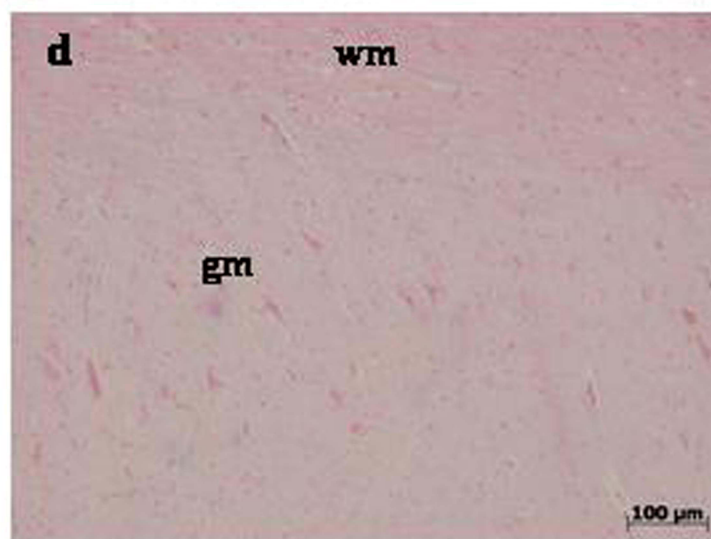
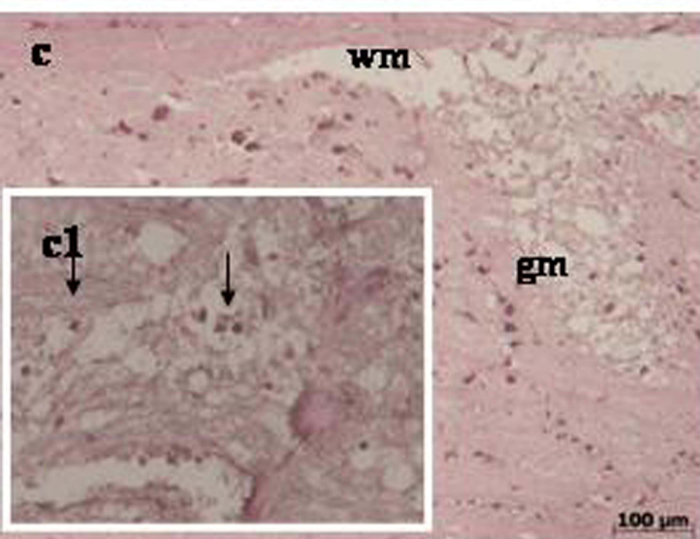
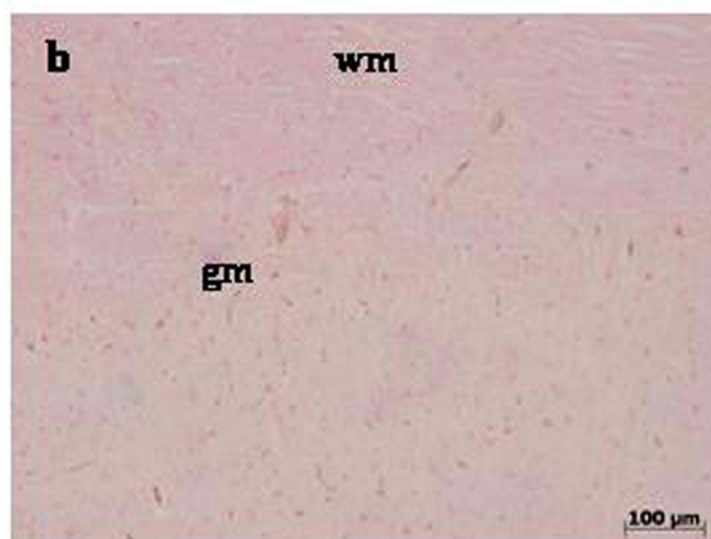
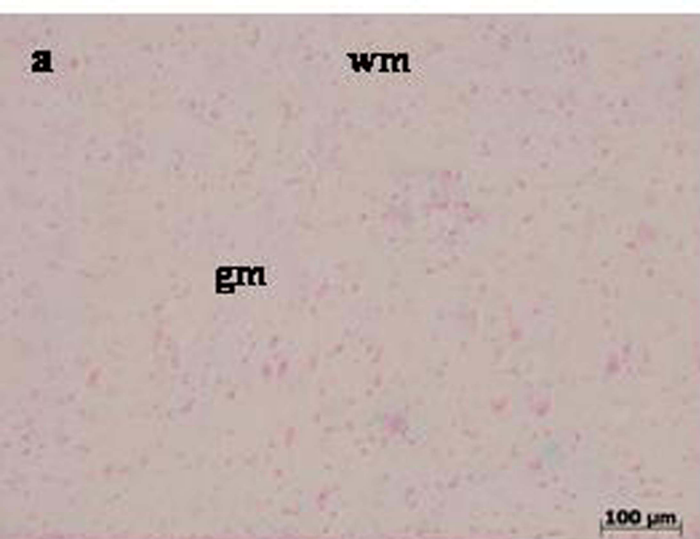


FIG.10

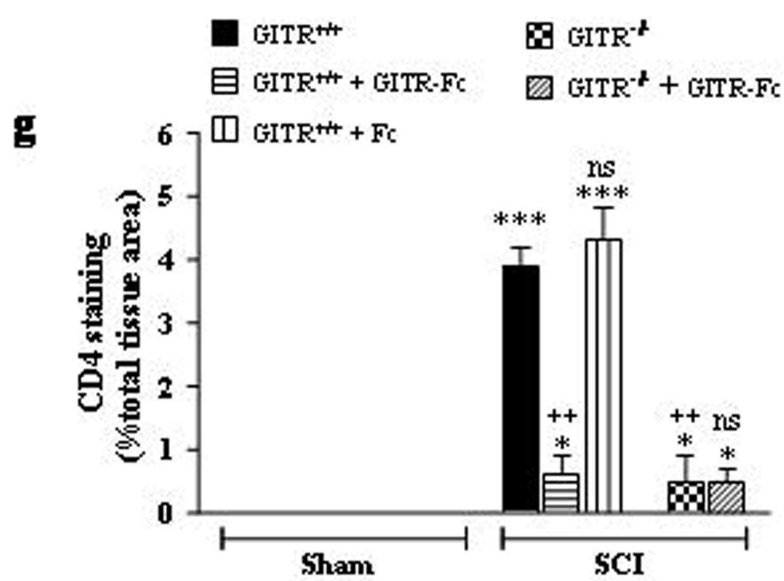


FIG.10

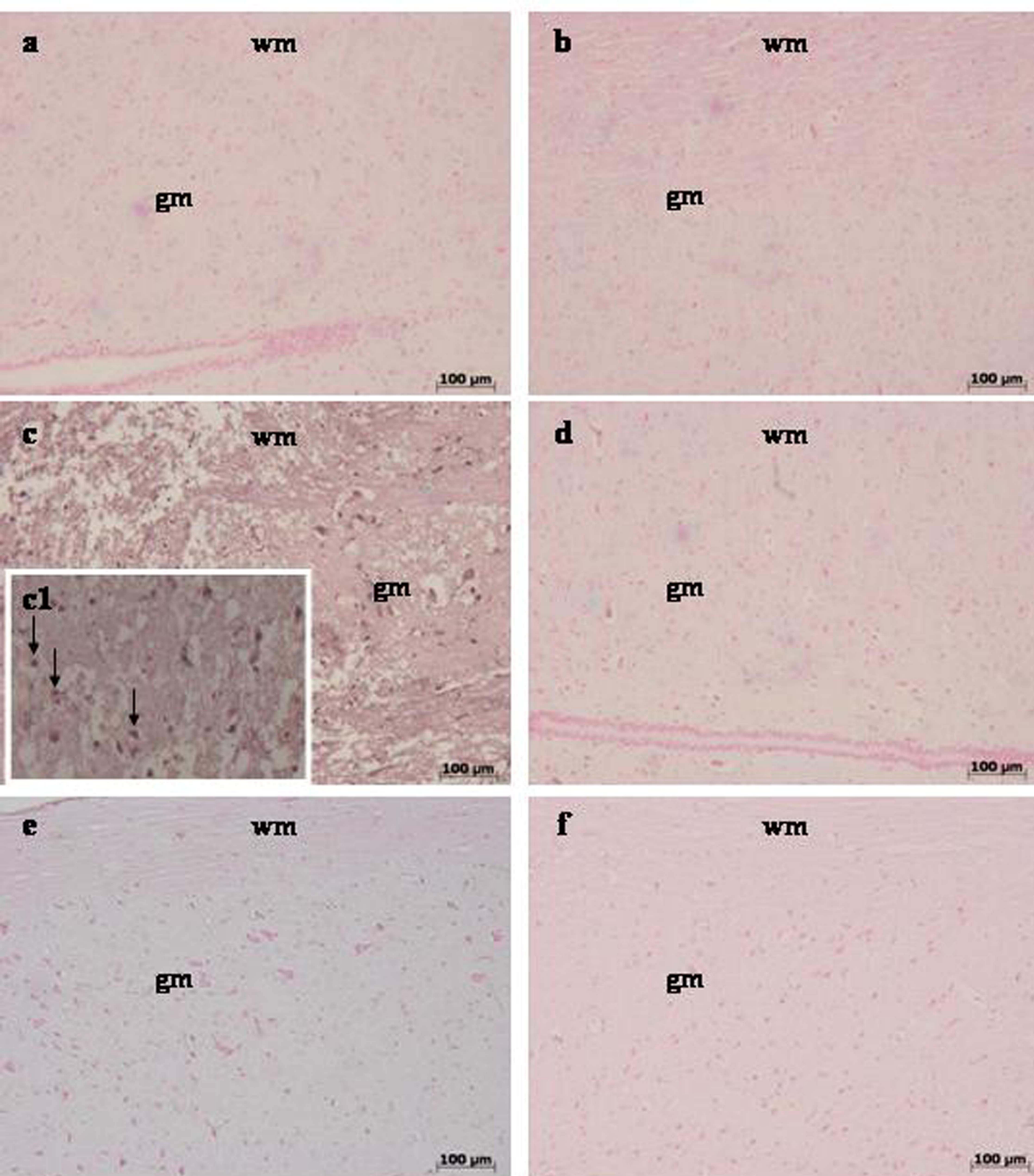


FIG.11

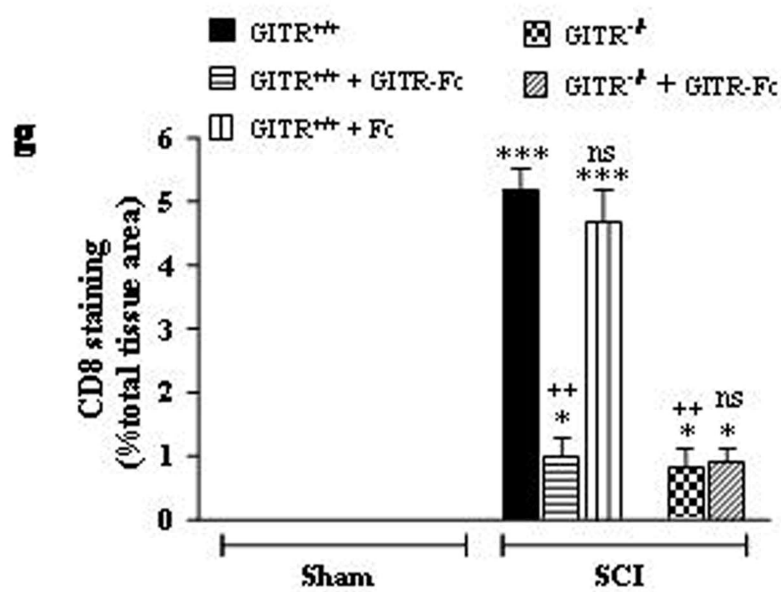


FIG.11